Pre-alpine mire sediments as a mirror of erosion, soil formation and landscape evolution during the last 45ka

Jäger, Hans ; Achermann, Matthias ; Waroszewski, Jarosław ; Kabała, Cezary ; Malkiewicz, Małgorzata ; Gärtner, Holger ; Dahms, Dennis ; Krebs, Rolf ; Egli, Markus

Abstract: Peat and lake sediments as well as a nearby soil catena were sampled to reconstruct the environmental history of a small infilled lake basin (mire) in the central alpine foreland of Switzerland. Soil evolution is best regarded as discontinuous over time and conceptualised by 'progressive' or 'regressive' process phases. We analysed the surrounding soils and used corresponding pedosignatures in the mire sediments to characterise notable phases of erosion and deposition. We assumed that the mire sediments would reflect these phases, that elemental composition (major and minor compounds) and rare earth elements (REEs) would allow us to differentiate past processes and that progressive and regressive phases of soil development can be discerned. Although radiocarbon ages are equivocal, it appears from pollen analyses that a lake was present here by c. 45 ka BP. After the retreat of the glacier from this area following the LGM, continuous sedimentation occurred until a mire developed during Pleistocene–Holocene transition. This transition period was accompanied by more intense erosion, as characterised by chemical signatures. A stable phase developed between c. 10–5 ka BP giving rise to progressive soil evolution. Between 5 and 4 ka BP, evidence appears for several erosional phases, predominantly detectable at the margin of the mire. These erosion phases, coupled with accumulation in the mire, are even more evident after 4 ka BP and especially after 2.1 ka BP. Based on soil investigations, elemental fluxes are detected along the slopes with distinct accumulations at the footslope. Evidence for anthropogenic influences and subsequent regressive soil formation phases appear in this pre-alpine landscape about 5 ka BP (Neolithic/Early Bronze Age), which appears to intensify after 2.1 ka BP (Roman period to present). Multi-elemental signatures enabled us to identify the important geochemical processes that have occurred here. Together with radiocarbon and pollen analyses, we placed these processes in a logical temporal context. The use of lacustrine (lake or mire) sediments has great potential to decipher and detail the surrounding landscape history and soil evolution of this region of Switzerland.

DOI: https://doi.org/10.1016/j.catena.2015.01.018

Originally published at:
Jäger, Hans; Achermann, Matthias; Waroszewski, Jarosław; Kabała, Cezary; Malkiewicz, Małgorzata; Gärtner, Holger; Dahms, Dennis; Krebs, Rolf; Egli, Markus (2015). Pre-alpine mire sediments as a mirror of erosion, soil formation and landscape evolution during the last 45ka. Catena, 128:63-79.
DOI: https://doi.org/10.1016/j.catena.2015.01.018

Pre-alpine mire sediments as a mirror of erosion, soil formation and landscape evolution during the last 45 ka

Hans Jäger[1)], Matthias Achermann[2)], Jarosław Waroszewski[3)], Cezary Kabała[3)], Małgorzata Malkiewicz[4)], Holger Gärtner[5)], Dennis Dahms[6)], Rolf Krebs[7)], Markus Egli[1)]*

[1)]Department of Geography, University of Zurich, Winterthurerstrasse 190, CH-8057 Zürich, Switzerland

[2)]Umwelt und Energie (uwe), Libellenrain 15, 6002 Luzern

[3)]Institute of Soil Sciences and Environmental Protection, Wrocław University of Environmental and Life Sciences, Grunwaldzka 53, 50-357 Wroclaw

[4)]Laboratory of Paleobotany, Department of Stratigraphical Geology, University of Wrocław

[5)]Unit Landscape Dynamics, Swiss Federal Research Institute WSL, Zürcherstrasse 111, CH-8903 Birmensdorf, Switzerland

[6)]Department of Geography, University of Northern Iowa, Cedar Falls, USA

[7)]Institute of Natural Resource Sciences, Zurich University of Applied Sciences, Wädenswil, Switzerland

* corresponding author: Tel.: +41 44 635 51 14; fax: +41 44 6356848.
E-mail address: markus.egli@geo.uzh.ch (M. Egli).

Abstract

Peat and lake sediments as well as a nearby soil catena were sampled to reconstruct the environmental history of a small infilled lake basin (mire) in the central alpine foreland of Switzerland. Soil evolution is best regarded as discontinuous over time and conceptualised by 'progressive' or 'regressive' process phases. We analysed the surrounding soils and used corresponding pedosignatures in the mire sediments to characterise notable phases of erosion and deposition. We assumed that the mire sediments would reflect these phases, that elemental composition (major and minor compounds) and rare earth elements (REE) would allow us to differentiate past processes and that progressive and regressive phases of soil development can be discerned. Although radiocarbon ages are equivocal, it appears from pollen analyses that a lake was present here by c. 44 ka BP. After the retreat of the glacier from this area following the LGM, continuous sedimentation occurred until a mire developed during Pleistocene-Holocene transition. This transition period was accompanied by more intense erosion, as characterized by chemical signatures. A stable phase developed between c. 10 – 5 ka BP giving rise to progressive soil evolution. Between 5 – 4 ka BP, evidence appears for several erosional phases, predominantly detectable at the margin of the mire. These erosion phases, coupled with accumulation in the mire, are even more evident after 4 ka BP and especially after 2.1 ka BP. Based on soil investigations, elemental fluxes are detected along the slopes with distinct accumulations at the footslope. Evidence for anthropogenic influences and subsequent regressive soil formation phases appear in this pre-alpine landscape about 5 ka BP (Neolithic/Early Bronze Age), which appears to intensify after 2.1 ka BP (Roman period to present). Multi-elemental signatures enabled us to identify the important geochemical processes that have occurred here. Together with radiocarbon and pollen analyses, we placed these processes in a logical temporal context. The use of lacustrine (lake or mire) sediments has great potential to decipher and detail the surrounding landscape history and soil evolution of this region of Switzerland.

Keywords: Mire sediments; soil evolution; erosion; dating; Quaternary

1. Introduction

In the European Alps, deglaciation had begun by 21 ka (Ivy-Ochs et al., 2006). As a result of the rapidly collapsing glacial cover at the end of the Late Glacial Maximum (Preusser, 2004; Schlüchter, 2004; Ivy-Ochs et al., 2006) a vast number of small melt water and kettle lakes formed in the Swiss Alpine foreland. Sediments filled most of these lakes afterwards via increased erosion and precipitation. Accordingly, mires began to develop on top of these sediments (Burga and Perret, 1998; Succow and Joosten, 2001). The accumulating lake silts, muds and peat layers trapped signals of the on-going landscape development and preserved them as environmental archives (Richardson and Vepraskas, 2001; Cohen, 2003; Chmieleski, 2006; Brisset et al., 2013). While peatlands have received much attention in the context of pollen and macrofossil analyses (Burga and Perret, 1998; Bennett and Willis, 2002; Birks, 2002), more recent approaches have focused on elemental analyses for pollution control and paleoclimate research (Lotter and Zbinden, 1989; Bindler and Klaminder, 2006; Franzén, 2006; Chapron et al., 2007). Less attention has been given to the analysis of pedosignatures contained in the surrounding landscapes (e.g. Mourier et al., 2010). Recent approaches have examined the links between mires and surrounding soils with a focus on defining pedogenic tracers in order to distinguish pedogenic processes geochemically and to relate them to mire sediments (Mourier et al., 2010; 2008; Brisset et al., 2013).

The Rare Earth Elements (REE) from La to Lu have been used for this purpose as small quantities of these are known to be widespread in soils (Öhlander et al., 1996; Aide and Smith-Aide, 2003; Franzén, 2006; Mourier et al., 2008). While REE in general are known to be mobile under the influence of weathering (Öhlander et al., 1996; Aide and Smith-Aide, 2003), the lighter members (i.e. La to Dy, also referred to as LREE) are particularly mobile and tend to fractionate amongst themselves. Thus,

74 subtle changes in the degree of LREE fractioning can be used to trace weathering and soil
75 formation/erosion as proxies for general landscape change (Mourier et al., 2008).
76 Several methods have been proposed to link sediments to their source(s) (Anda et al., 2009; Stutter et
77 al., 2009 or Mondal et al. 2012). Mondal et al. (2012) derived a set of oxides and elements from
78 sedimentary material and normalized it with standard Upper Continental Crust (UCC) material (see
79 Taylor and McLennan, 1985). They then compared the pattern of average REE contents after
80 normalizing them with a Chondrite standard (Sun and McDonough, 1989). Other methods have used
81 the carbonate content and concentrations of selected elements and/or weathering indexes to compare
82 soils and to identify certain chemical alterations within them (e.g., Cohen, 2003; Franzén, 2006; Le
83 Roux and Shotyk, 2006; Egli et al., 2008; Adams et al., 2011; Buggle et al., 2011 etc).
84 The main objective of our study was to reconstruct the soil and environmental history of a small
85 infilled lake basin in the glacial foreland of central Switzerland. We used pedosignatures in lake and
86 mire sediments as defined by Mourier et al. (2008, 2010) and Mondal et al. (2012) (weathering
87 parameters, REE signatures) to characterise the history of soil genesis, chemical weathering and
88 erosional variability. We used the following hypotheses: 1) mire sediments reflect the soil forming
89 processes of the surrounding area and give a relatively detailed insight into phases of weathering and
90 erosion; 2) total elemental composition and REE can be used to trace past environmental processes; 3)
91 using this approach, progressive and regressive soil forming phases can be recognised.
92
93 **2. Materials and methods**
94 *2.1. Study area*
95 The sampling site Moosried (540 m a.s.l.) is a protected fen (minerotrophic mire) listed in the federal
96 inventory of mires with national importance, near the village Adligenswil in the Würzenbach valley
97 (canton of Lucerne) at the margin of the Swiss Alps (Fig. 1). The mire and its underlying sediments
98 developed on top of a former proglacial lake which has infilled over time. This location was buried

99 under approximately 500 m of ice during the Last Glacial Maximum (LGM) and has experienced
100 several advances and retreats of the ice front during the Late-glacial prior to the large-scale ice-collapse
101 episode(s) of the Bølling and Allerød interstades (Burga and Perret, 1998; Hantke, 1980, 2011;
102 Schlüchter, 2004; Preusser, 2004; Ivy-Ochs et al., 2006; Preusser et al., 2011). A remnant moraine is
103 present at Stöcke, just south of Moosried, that indicates that a lobe of the Reuss glacier stopped there
104 on its last advance before 17000 cal BP but did not reach the sampled area again (Hantke, 2011).
105 Examinations of the nearby slopes of the Meggerwald region show that soil formation must already
106 have started at least on the slopes of the valley by 18000-to-19500 cal BP (Egli et al., 2010).
107 The Moosried fen is flanked by SW-to-NE-trending slopes. Like the valley basement they consist of
108 folded subalpine molasse originating from the c. 23 Ma Chattian/Aquitanian (Untere Süsswasser
109 Molasse). The molasse in this region consists of a granitic sandstones with a high content of feldspar
110 and of sporadically occurring marly or clayey layers. In addition, the southern valley slopes show
111 repeated layers of conglomerates consisting of mostly crystalline clasts (and sporadic clasts of flysch
112 origin) embedded in a sandstone matrix (Nagelfluh) (GKSNG and Swisstopo, 1962; Hantke, 1967;
113 BWG, 2006).
114 The modern landscape between the lakes of Lucerne and Zug is shaped by erect molasse plates and the
115 numerous troughs between them which feature numerous mires (Hantke, 2011). Mean annual
116 precipitation is c. 1300 mm and mostly occurs as rainfall in summer. Mean monthly temperatures range
117 from -1 ºC in January to 18 ºC in July. The potential natural vegetational cover has been replaced by
118 *Picea abies*-dominated forests on the southern valley slopes while the bottom of the valley and its
119 northern slopes are mostly under agricultural use. Cambisol-type soils (IUSS working group WRB,
120 2007) prevail on the bottom of the valley and on its northern slopes, while Dystric Cambisols most
121 often occur on the forested southern slopes and in some areas even signs of advanced podsolization can
122 be found (Egli et al., 2002). Gleysols and Histosols are found in the waterlogged parts of the valley
123 bottom.

The mire itself may have been used in the past as pasture and for straw litter, as these were common in such areas (Mühlethaler, 2002). From the 1940s to the 1960s it has in part been used for potato cultivation (Röösli et al., 2004). Some peat cutting was done during World War I, and the mire was used only to store peat cut from a nearby mire during World War II (Probst, 1922; Röösli et al., 2004). Although this mire underwent some peat cutting and agricultural use and has been exposed to some drainage and earthwork, it is considered to be in a surprisingly natural state and is now mainly covered in sedge reeds, poor grassland and wet meadows (Röösli et al., 2004).

The differentiation of peat types is according to Rydin and Jeglum (2006) and Succow and Joosten (2011) while the classification of organic rich lake sediment follows the suggestion for Central Europe according to Chmieleski (2006). Elemental concentrations (e.g., Boyle, 2002; Le Roux and Shotyk, 2006) are used to distinguish between layers and to characterise them.

2.2. Sampling strategy

We sampled the peat and lake sediments at Moosried fen as well as three soil profiles (Fig. 1, Table 1). The three soil profiles were excavated along a NW-facing hillslope catena in the nearby forest (Fig. 1; P1-3): one at the shoulder, one at mid-slope and one at the footslope. Undisturbed cylinder samples were taken from all soil horizons – and where applicable rock samples – were collected to determine bulk density. In addition, approximately two kilograms of soil (cf. Hitz et al. 2002) was collected per horizon for having a representative soil sample (that also enabled the determination of the soil skeleton proportion). Five sediment cores were obtained in the area within the mire. Cores were sampled from the centre to the margin at locations A, B, C, and E using a Humax rotating drill. Samples were obtained at locations BII (the lower part of core B) and G with a Russian side-opening sampler (Macaulay). For the core EXK only the peat base was sampled with an auger sampler for dating purposes. Core E had to be repositioned as an abandoned drill in direct line was blocked by clasts in the underground from the nearby small stream.

149

150 *2.3. Chemical and physical analyses*

151 Oven-dried samples (70 ºC) were sieved to < 2 mm (fine earth) and homogenised with a sample
152 separator (Rentsch PT 1000). The bulk density (fine earth and soil skeleton) was measured on
153 undisturbed samples (volumetric sampling using the corers and cylinders). Soil, sediment and peat pH
154 (0.01 M $CaCl_2$) was determined for 60 fine earth samples using a soil:solution ratio of 1:2.5. Loss on
155 ignition (LOI) was measured for 110 samples on 1.5 g oven-dried and milled (< 63 µm) fine earth,
156 ignited at 950 °C for 2h. Measurement of the total element content was done by energy dispersive X-
157 ray fluorescence (ED-XRF). Approximately 10 g of material were milled to < 63 µm in a tungsten
158 carbide disc swing mill (Retsch® RS1, Germany). 110 powder samples of approximately 5 g material
159 were analysed using an energy dispersive He-flushed X-ray fluorescence spectrometer (SPECTRO X-
160 LAB 2000, SPECTRO Analytical Instruments, Germany). LOI directly gave a good estimate for
161 organic matter there where no carbonate was present. Distinction between inorganic and organic C was
162 done (for the samples containing carbonates) using the LOI values (that includes both organic matter
163 and carbonates) and Ca and Mg concentrations, summing them as CaO, $CaCO_3$, MgO and $MgCO_3$ and
164 adjusting these compounds together with organic matter iteratively to LOI and, together with the other
165 main elements in oxide form, to 100%.

166

167 *2.4. Weathering indices*

168 Weathering characterization is based on the calculation of elemental losses from soil or sediment
169 profiles. Element specific gains and losses are determined using enrichment/depletion values
170 determined from concentration profiles of immobile elements such as Ti or Zr. Weathering rates can be
171 calculated when the ages of landforms are known (Chadwick et al., 1990; Egli and Fitze, 2000). The
172 assumption is that the weathering profile has developed from a homogeneous parent material. This is
173 approximately true for our soil profiles but obviously not for the different strata of the mire sediments.

Relative elemental losses can be calculated using the open-system mass transport function $\tau_{j,w}$ (Chadwick et al., 1990):

$$\tau_{j,w} = \left(\frac{C_{j,w} \cdot C_{i,p}}{C_{i,w} \cdot C_{j,p}} \right) - 1 \quad (1)$$

where i denotes the immobile element (Ti), $C_{j,p}$ (g/kg) is the concentration of element j in the unweathered parent material, $C_{j,w}$ is the concentration of element j in the weathered product (g/kg). Mourier et al. (2008) showed that Rare Earth Element (REE) geochemistry of lacustrine sediments and soils is useful for reconstructing the history of landscape evolution. Normalised REE patterns may thus provide a precise tracer of the degree of weathering of materials. Consequently, the REE concentrations were normalised to a chondritic reference standard (Sun and McDonough, 1989) to facilitate the comparison of REE patterns between sites. Normalisation against a common reference helps to identify subtle fractionations and anomalies in elemental abundances (Mourier et al., 2008). Only a portion of the REEs could be measured using XRF (La, Ce, Pr, Nd and Sm). Consequently, the sample composition also was compared to a set of major and trace elements according to Mondal et al. (2012) – which was normalised to a revised UCC-standard (Upper Continental Crust) (Taylor and McLennan, 1995). This set includes SiO_2, TiO_2, Al_2O_3, Fe_2O_3, CaO, MgO, Na_2O, K_2O, MnO, V, Cr, Ni, Cu, Zn, Rb, Sr, Y, Zr, Nb, Ba, Pb, Th und U.

2.5. DRIFT measurements

Relative peak intensities were used for DRIFT analysis (Bruker, Tensor 27). Spectra were recorded from 4000 to 250 cm^{-1} using a powder containing 9-12 mg of sample (3% of the total weight) and 291-388 mg KBr (97% of the total weight). Prior to measurement, the samples were again oven-dried at 60° C. The FT-IR spectra of 42 oven-dried and milled (< 63 µm) fine earth samples were interpreted using the OPUS 6.5 software.

199

200 *2.6. Plant macrofossils*

201 In several portions of the peat and sediment profiles, plant relics were detected and analysed (Birks,
202 2002). This was done with a binocular and / or a microscope using thin sections created with a
203 specialised microtome (Gärtner et al., 2014). A total of 3 mire profiles were analysed. Using tangential,
204 radial and cross-sections, the macro rests were characterised by distinguishing between coniferous and
205 deciduous tree or shrub remnants (Schweingruber, 1990, 1996). No further classification was possible
206 due to the heavy deformation and alteration of the available remnants.

207

208 *2.7. Pollen analysis*

209 Twenty samples (total) were taken from the cores B and G. Sixteen samples were collected from core B
210 at a depth of 35-40, 60-65, 110-115, 135-140, 160-165, 170-175, 210-215, 275-284, 335-344, 390-399,
211 453-463, 467-476, 505-513, 567-576, 617-626 and 685-695 cm. In core G, samples were taken at
212 depths of 403-413 and 704-713 cm to check for the presence of pollen and, furthermore, at the depth of
213 121-130 and 180-189 cm. Organic (peat) samples were heated in a 10% KOH solution to remove the
214 humified organic matter; the mineral samples were treated using 40% HF to dissolve siliceous minerals
215 (Faegri and Iversen, 1989). Following this step, cellulose was destroyed using acetolysis (Erdtman,
216 1960). 400-1000 sporomorphs were counted in each sample on 2-4 glass slides. Pollen grains were
217 detected only in the upper section of the gyttja of G core (121-189 cm; no pollen was found at 403-413
218 and 704-713 cm), thus the further calculations for pollen spectra were done for the B core only. Based
219 on the abundance of individual species or groups of taxa, the percentage of arboreal (tree species) and
220 non-arboreal (shrubs and herbaceous species) pollen was derived. Cryptogams were excluded from the
221 sum of the grains. The palynological software POLPAL was used to prepare the pollen diagrams
222 (Nalepka and Walanus, 2003).

223

224 *2.8. Radiocarbon dating of organic matter fractions*

225 Organic samples were cleaned using an acid-alkali-acid (AAA) treatment. The samples were then
226 heated under vacuum in quartz tubes with CuO (oxygen source) to remove any absorbed CO_2 in the
227 CuO. The tubes were then evacuated, sealed and heated in the oven at 900 °C to obtain CO_2. The CO_2
228 of the combusted sample was mixed with H_2 (1:2.5) and catalytically reduced over iron powder at 535
229 °C to elemental carbon (graphite). After reduction, the mixture was pressed into a target and carbon
230 ratios were measured by Accelerator Mass Spectrometry (AMS) using the tandem accelerator of the
231 Laboratory of Ion Beam Physics at the Swiss Federal Institute of Technology Zurich (ETHZ). In
232 addition, two inorganic samples (carbonates) from lake sediments (one at the transition between lake
233 sediment and bedrock) were dated.

234 The calendar ages were obtained using the OxCal 4.1 calibration program (Bronk Ramsey, 2001, 2009)
235 based on the IntCal 09 calibration curve (Reimer et al., 2009). Calibrated ages are given in the 2σ range
236 (minimum and maximum value for each).

237

238 **3. Results**

239

240 *3.1. Surrounding soils*

241 The uppermost profile (#1), is a Dystric Cambisol that exhibits an O-AE-Bsw-BC profile over bedrock
242 with relatively strong podzolic features (Tables 1–2). The bedrock consists of granitic sandstones
243 (widespread in the area) with a high feldspar content (arkose). The sandstone usually includes layers of
244 conglomerate consisting of mostly crystalline clasts. Several granitic clasts are found throughout the
245 profile. This profile features the highest skeleton content of all profiles with about 20% in the B
246 horizons with bulk density strongly increasing in the BC horizon. The pH of the topsoil is highly acid
247 (3.25) with increasing values towards the BC horizon (5.0; Table 2). Although LOI only gives an

248 estimate of soil organic matter, it indicates a rapid downward decrease in the content of organic
249 material to the B-horizons (Table 2).
250 The mid-slope profile (#2) also is a Dystric Cambisol that exhibits a O-AE-Bws-Bw-BC profile (Tables
251 1-2). In this profile the AE horizon is only slightly bleached and the Bws horizon, while still enriched
252 in sesquioxides (as also shown by the soil colour; Table 2), is more weakly developed than in profile
253 #1. The Bw horizon gradually changes into a sandy BC horizon of pale colour. The skeleton content
254 does not exceed 5% in this profile and shows smaller clasts than in profile 1. Bulk density clearly
255 increases to the B horizons. The pH remains acidic throughout the profile. Fe, Al and Si contents
256 generally increase with depth (Table 3) while LOI strongly decreases (Table 2). DRIFT results showed
257 a higher content of kaolinite (peaks at 3692 and 3622 cm^{-1}) in the upper horizons while the amounts of
258 mica (3624 and 531 cm^{-1}) decrease. Traces of quartz (doublet at 780 and 800 cm^{-1}), vermiculite (802
259 cm^{-1}) and smectite (690 cm^{-1}) were present in all horizons (Fig. 2).
260 The footslope profile (#3) is a Gleysol located at the edge of a wet meadow that exhibits an A-B1-Cr
261 profile. This profile clearly shows the influence of subsurface meteoric water movement. The A
262 horizon has a considerable amount of organic matter (Table 2), but no skeleton material. Changing
263 redox conditions are macromorphologically observed in the Bl horizon while The Cr horizon has a
264 greenish-greyish colour typical of reducing conditions. The soil matrix is sandy and bulk density
265 abruptly increases below the A horizon. The pH values varies from 5.10 in the A to 6.45 (Table 2) in
266 the Cr. Al increases with depth but almost no change was measured for Fe (Table 3).
267 DRIFT analyses showed a general decrease of smectite minerals in the topsoils of this catena from the
268 uppermost (shoulder) to the lowermost (footslope) site, while recording an increase in mica (data not
269 shown). The visual and analytical evaluation of the profiles clearly shows more extensive weathering
270 and acidification with increasing (higher) slope position.
271
272 *3.2. Mire cores*

273 Core E is situated at the margin of the mire close to the slope (Fig. 1) where the soil profiles were
274 described. The core showed slightly acidic conditions throughout its extent and therefore contained no
275 carbonates (Fig. 3). Due to the marginal position of core E in the mire, the organic matter content was
276 not particularly high and inorganic material was admixed. The pH stayed between 5.5 and 6 throughout
277 the core. LOI showed the expected decrease in the first 100 cm (Fig. 4) while bulk density tended to
278 increase to about 3 m depth (Fig. 3). Under a loamy topsoil layer, the soil changes to sandy material
279 containing several clasts and grades to finer sand with a far lower clast content at 255 cm depth. At 150
280 cm depth, we see a noticeable increase in glittering mica and fine quartz. At the time of sampling, the
281 water table was just below the core, at 300 to 350 cm. At 330 cm, the amount of rounded clasts
282 increases again. The material composition corresponds well to that of the soil profiles' BC horizons
283 (Fig. 4, Table 3). The SiO_2 content mostly ranged between 60 and 70% (in the BC horizon between 64
284 and 68%) and the Al_2O_3 concentration between 12 and 17% (in the BC horizon between 14.7 and
285 16.3%). The SiO_2 and Al_2O_3 content throughout the core showed no peculiarities. Al_2O_3 exhibited a
286 minor increase at 250 cm at the position where the sand becomes finer.
287 Core C is situated within the mire (about half the way to the centre; Fig. 1). A loamy topsoil changes to
288 woody peat from 55 cm to 100 cm. This peat contains large woody macrorests from roots, branches or
289 other tree and shrub remnants. At 125 cm the colour of the peat becomes darker and macromorphology
290 shows signs of increased decomposition. The transition from the topsoil to the peat also is clearly seen
291 in the LOI depth trend, bulk density, and mineral indicators (Figs. 3 and 4). The pH values gradually
292 increases with depth from about 5 to nearly 7 (Fig. 3). Such values are often encountered in carbonate
293 bearing fens (Rydin and Jeglum, 2006) and may point to the influence of subsurface runoff from the
294 surrounding slopes. The prominent layer of sandy muck (mud) from 230 cm to 250 cm is represented
295 by changes in bulk density (Fig. 3), LOI (Fig. 4) and the mineral indicators SiO_2 and Al_2O_3 (Fig. 4). At
296 about 250 cm the woody peat reappears and at 275 cm another, even thicker, layer of coarse sandy
297 muck is found that changes again to woody peat at about 325 cm. These changes were again mimicked

298 by the LOI, bulk density and mineral contents (Figs. 3 and 4). The base of the peat appears to occur at
299 350 cm at the appearance of a very pale layer of limey gyttja containing an abundance of snail shells.
300 Core A is situated closer to the centre of the mire (Fig. 1). Core A is somewhat shorter as the drilling
301 was refused at about 260 cm due to of a large piece of wood. A loamy topsoil changes to woody peat at
302 about 50 cm – which again contains large macrorests.
303 Cores B (Humax drill to 220 cm) and BII (Macaulay from 257 cm to depth) are from the centre of the
304 mire (Fig. 1). The drilling stopped at about 700 cm due to decreasing sediment consistency and
305 difficulties with the Macaulay drill. The transition from the uppermost layer to peat occurs about 55 cm
306 which is also reflected in the bulk density (Fig. 3), LOI (Fig. 4) and detrital elemental contents. The
307 uppermost layer shows remnants of a sedge peat that is different from the woody peat beneath (Fig. 4).
308 Macrorests of a spruce (*Picea abies (L.) Karst)* root fragment were found which showed well-formed
309 frost rings and signs of mechanical impacts (40 – 50 cm depth; Fig. 5). The pH values varied between 5
310 in the upper core and 7 at the peat base at about 370 cm at the gyttja interface (Fig. 3). The
311 macromorphology of the cores indicates higher degrees of peat decomposition at 100 cm and at 250
312 cm. At 250 cm the woody peat changes to a layer of sedge peat (giving rise to a slight change in bulk
313 density; Fig. 3) to 330 cm where the first layer of organic gyttja is encountered. As before, the
314 transition from peat to gyttja can be seen in the LOI, pH values and detrital elemental concentrations
315 (Figs. 3 and 4). Bulk density does not follow this pattern at this location, as it decreases to the subsoil
316 then slightly increases again with the gyttja layers without showing any distinct change. From 340 cm
317 to 370 cm another layer of sedge peat is found that marks the peat base that is then underlain by a 200
318 cm+ thick horizon of organic gyttja from 370 cm to 600 cm. The organic gyttja contains many weed
319 remnants and clamshells and the pH value increased to 6.5 (Fig. 3). Beneath this layer, the sediment
320 again changed to a pale and layered limey gyttja.
321 Core G is situated only a few meters southwest of B/ BII in the middle of the mire (Fig. 1). Again, a
322 layer of woody peat appears at about 50 cm with increased signs of decomposition from about 80 cm to

323 the peat base at 100 cm (as reflected also by the bulk density; Fig. 3). At this point a bright white layer
324 of varved lake marl appears, containing many snail shells, some weed remnants and some small
325 rounded clasts. This marl changes to marly silt sediment at about 200 cm (reflected by the SiO_2 and
326 Al_2O_3 content; Fig. 4). The abundance of snail shells decreases abruptly here, but some individual weed
327 remnants are still present in the top layers together with a few clamshells. Another significant change in
328 sediment composition appears at about 360 cm where organic remains nearly disappear from the core
329 (Fig. 4). Upon drying, the core easily fell apart into its varved components (very thin clayey-silt layers,
330 each of it separated by a slightly coarser sand layer between them). In these varves non- or only
331 slightly-rounded clasts are encountered of larger size than in the sediment above. Angled quartz
332 fragments appear at 590 cm, along with a slightly rounded dark piece of limestone and an angled
333 broken gneiss fragment, showing a high content of mica – a kind of 'erratic' rock debris which is not
334 typical for the region today (consequently something that was transported there by the glacier). These
335 appear to be almost entirely 'clastic' varves with very small amounts of biogenic material.
336 At 470 cm, a very coarse layer of sand is found. It is the most prominent but not the only evidence of
337 the overwhelming clastic detrital input in this core. The end of the core was reached at 710 cm due to
338 the presence of larger clasts that apparently mark the base of post-glacial sedimentation at this position
339 in the basin. While LOI values clearly show the transitions from lake marl to marly silt to clayey silt
340 (Fig. 4), the pH values are more equivocal, with values ranging from 7.3 to 8.0 (Fig. 3). Bulk density
341 variations indicate a continuous increase in density with depth, regardless of the differing sediment
342 units (Fig. 3). The content of detritus indicator-elements such as SiO_2 or Al however, clearly show
343 well-expressed changes (e.g., a doubling of the SiO_2 content from marly silt to clayey silt; Fig. 4).
344 DRIFT results indicate much less kaolinite and a corresponding increase in mica and vermiculite from
345 the marly silt to the clayey silt (Fig. 2).
346
347 *3.4. Radiocarbon dating*

348 A total of 11 samples were dated (Table 4). In contrast to the organic materials analysed from cores B,
349 BII and C and the peat base of core G (wood, peat, organic remnants in gyttja), we were forced to rely
350 on lake carbonates for age analyses of core G. Ages of about 44500 cal BP and 42000 cal BP were
351 initially obtained from the carbonate gyttja (Table 4; Fig. 6). In a second attempt, we analysed organic
352 microrests from adjacent layers; these samples provided a clearly younger age of about 12700 cal BP
353 and 10500 cal BP. However, rather strange $\delta^{13}C$ values were measured for these samples (about -46‰
354 that is possibly due to the influence of methano-bacteria).
355 The ages for the organic materials in cores B, BII and C and the peat base of core G appear reasonable
356 while the results from the lake sediment in core G are not easily explained (Table 4). At the centre of
357 the mire, the peat base of core BII exhibits the initial appearance of sedge peat at about 11000 cal BP
358 (Table 4, Fig. 6). The limey gyttja beneath the sedge peat has a similar age (10500 cal BP). Together
359 with the thickness of the more organic gyttja above, this points to the presence of an inward growing
360 floating mat on a lake while younger organic material is still incorporated into the underlying gyttja as
361 long as there was water present between the floating mat base and the gyttja. This suggests that initial
362 peat growth started earlier near the lake margin. That the first 40 cm has a degraded and partially
363 humified peat points to an anthropogenic influence. The base of the peat in core G yields an age of
364 about 9500 cal BP (Fig. 6); thus it must have followed directly on top of lake marl since no additional
365 organic layers are found beneath it.
366 At site C the peat started to accumulate rapidly by 5300 cal BP until about 4000 cal BP (Fig. 6), when
367 the formation of pure peat was replaced by repeated pulses of detrital sediments.
368
369 *3.5. Pollen analysis*
370 Based on the pollen spectra (Fig. 7), three different sections can be distinguished in core B. The bottom
371 section, from 695 up to 617 cm (within the calcareous gyttja), is clearly dominated by arboreal pollen,
372 in particular those of deciduous species such as *Corylus* sp. *(decreasing to the top)*, *Alnus*, *Ulmus* sp.,

373 *Quercus* sp. and *Tilia* sp. *(all three stable throughout the section)*. Some admixture of other
374 broadleafed species can be recognised such as *Betula* sp., *Fraxinus* sp., *Acer* sp. and *Salix* sp.. *Pinus*
375 *sylvestris* L. is detectable, but its small percentage may be due to long-distance transport. At about 626
376 cm, the pollens of *Picea abies* and, in particular, of *Abies alba* Mill. appear. Pollen of *Hedera helix* are
377 also present. The proportion of herbs (*Poaceae*, *Cyperaceae*, *Rosaceae*) does not exceed 4% and so
378 testifies to a stand of closed forest.
379 The section between 576 cm and 135 cm initially contains an equal share of arboreal and non-arboreal
380 pollen, with the non-arboreal types gradually decreasing upward in the core (Fig. 7). *Abies* and *Alnus*
381 prevails in the tree pollen, while *Betula* pollen rapidly increases at 210 cm. The proportion of *Corylus,*
382 *Ulmus, Quercus* and *Tilia* pollen is significantly lower when compared to the basal section. The new
383 species is *Fagus sylvatica*. When starting from 335 cm, the share of non-arboreal pollen (NAP)
384 increases up to 50%.
385 The uppermost section (115 to 35 cm) indicates a progressive increase of moister conditions,
386 manifested by the increasing proportion of *Alnus* pollen, *Sphagnum* spores and the presence of
387 *Selaginella* (spike mosses). There is also a slight but continuous increase in *Abies* and *Picea abies,*
388 while *Betula* and *Filicales* decrease. Noteworthy is the presence of *Hedera helix*. With respect to the
389 *Poaceae*, some *Cerealia* were detected. These suggest increasing human impacts in the region (due to
390 agriculture).
391 A slightly different pollen composition was noted in the G core section, with a dominance of *Betula* at
392 180-189 cm and an increase in *Betula* and *Pinus* at 121-130 cm depth. The presence of *Salix,*
393 *Hippophae, Chenopodiaceae, Artemisia* and *Helianthemum* indicated a more open space areas. The
394 NAP content was between 10 to 20%.
395
396 *3.6. Rare earth elements and UCC normalised elemental contents*

We used a set of major and trace elements to assess the detrital input into the mire Mondal et al. (2012). The elements were normalised using an upper continental crust (UCC) standard (Taylor and McLennan, 1995) and a set of measurable REE was compared to it (Mondal et al., 2012; Stutter et al., 2009) after normalisation to a chondrite standard (Sun and McDonough, 1989; Table 5). The resulting values of the chondrite-normalised measureable REE were all similar (Table 5) and no particular trend can be detected.

The variation of the UCC-normalised contents of major and minor compounds among the BC horizons of the soil profiles is very small (indicating the homogeneity of the parent material). In Figure 8, several sections of the mire cores are compared to the BC horizon of profile 2 (as the soil parent material indicator). The sandy muck of core C is directly linked to the soils' parent material due to their high similarity. A relatively good correlation of the sand in core E to the soils' parent material is evident (Fig. 8). A weaker relation, however, is present between the soil parent material and the gyttja of core B while the clayey silt of core G and the limey gyttja of core C seem to have an altogether different signal.

4. Discussion

4.1. Soils

The open-system mass transport functions τ for the major elements of the soils are shown in Figure 9. Negative values (and thus losses) of the main elements appear in the upper horizons; with increasing depth, these values become less negative. The open-system mass transport functions typically show elemental fluxes (via subsurface flow) along the slope of the catena (P1 → P2 → P3). The losses at P1 are much more pronounced than at P3. Mobilization of Fe appears to be active in the upper portion of the catena whereas accumulation dominates at the lower position – an effect that has been termed 'lateral podzolisation' (Sommer et al., 2001). A similar effect both within the soil profile and along the slope can be detected for the rare earth elements (REE) La, Ce, Pr, Nd and Sm. The relations among

these elements clearly indicate the lateral transport of detritus and chemical compounds along the slope and into the mire (Fig. 10). It has been shown that soil development started at nearby sites at least about 18000 cal BP (Egli et al., 2010) and that weathering has led to the formation of Dystric Cambisols and even Podzols (Egli et al., 2002). Soil profiles 1 and 3 fit well in this system. Egli et al. (2002) showed that the molasse sandstone contains smectites and that due to the converse behaviour of mica and chlorite in these soils, it is possible to trace the neoformation of smectite back to the weathering of these minerals. The smectites were identified as rather low-charge minerals with a predominance of montmorillonite and mixed phase montmorillonite-beidellite (Egli et al., 2002). Kaolinite and vermiculite also are present and although the clay mineral analyses for the present study are less comprehensive, similar mechanisms should be expected for soil profiles 1 and 3. However, at the mire's margin, profile 3 clearly shows the influence of subsurface water and a subsequent lateral input.

4.2 Element fluxes and detrital inputs into the mire

The UCC-normalised elements indicate that several mire profiles are directly related to the surrounding soils: sandy material of the cores C and E can be traced back to soil material input and the gyttja of core B was partially influenced by eroded and deposited soil material. Consequently, their evolution is related to slope processes. The clayey silt of core G and the limey gyttja of core C, however, were less influenced by erosional processes from the slopes. In particular, the deep sediment layers of core G point to a different genesis than that of core C. This can be seen by the angled rock fragments and thick silt layers with coarse sand inputs within the clastic varves.

'Progressive' soil development is generally assumed to be the result of a combination of chemical and physical weathering and mineral transformation, while 'regressive' soil development primarily is led by erosion (Johnson and Watson-Stegner, 1987; Sommer et al., 2008; Egli and Poulenard, 2014). Changes in soil forming factors may be very abrupt, either by catastrophic natural events (erosion) or by human influence (land use change, intensification of agriculture; Egli and Poulenard, 2014). The

447 patterns of the UCC-normalised elements point to erosional and, consequently, regressive phases of
448 soil evolution. With increasing distance from the adjacent hillslopes (the distance is: E < C < BII; Fig.
449 8), the general trend of the major compounds is toward a more depleted elemental composition
450 compared to the soils' parent materials. Finer (and thus more strongly-weathered) sediments were
451 transported the furthest. In addition, the differences in Ni and Cr seem to be systematic in core E, BII
452 and G with respect to the BC horizon of soil P2 (Fig. 8). We speculate that this is not only due to
453 differences in the lithological substrate but that it is an indication of mass flux from the slopes towards
454 the middle part of the mire. We assume that this transport is the result of groundwater and subsurface
455 flow along the slopes. The enrichment of Cr and Ni at the footslope relative to P2 appears to support
456 this assumption (Fig. 8). Furthermore, if the open-system mass transport functions are plotted (data not
457 shown) we see the fluxes of Cr and Ni along the slope in a pattern similar to the major compounds (Fig.
458 9). In addition, chromium chemistry is related to a certain degree to the Fe- (Stanin and Pirnie, 2004)
459 and Mn-chemistry (Guha et al., 2001) which strongly depend on the redox situation (particularly
460 relevant for groundwater transport). The mobility of Ni is governed by soil organic carbon and,
461 similarly to Cr, by the behaviour of Fe-Mn sesquioxides (Rinklebe and Shaheen, 2014).
462 By normalizing rare earth element concentrations (e.g. to chondrite or immobile elements), enrichment
463 or depletion of REE fractions can be observed relative to the unweathered source material (Mourier et
464 al., 2010). REE patterns in soils are modified during pedogenesis (Öhlander et al., 1996; Aide and
465 Smith-Aide 2003; Mourier et al., 2010), and REE elemental fractionation occurs. Specific minerals
466 have distinctive affinities for the individual REEs (Mourier et al., 2010), so REEs are often complexed
467 with carbonates, organic matter or phosphates, or adsorbed onto clays and Fe- and Mn-oxyhydroxides
468 (Aide and Smith-Aide, 2003). REE fractionation and leaching is stronger in acid soils (e.g., Ingri et al.,
469 2000). Thus, low REE values indicated an increase in weathering and high REE values indicate a
470 decrease. High values are related to stable phases; i.e. the deposition of lake sediments or the formation
471 of the peat (that showed the most positive values). Detrital input that show similar patterns is detected

472 at 100 cm, 150 cm and 200 – 250 cm in cores A and C (Fig. 10). At the margin of the mire, profile E is
473 influenced predominately by slope deposits on which a shallow mire has developed. Due to their
474 position toward the middle of the mire, cores B and G mainly exhibit features of a more or less
475 undisturbed peat development. The inputs of solutes and solid materials from the nearby slopes are
476 clearly decreased here, with increasing distance from the mire margin and, consequently, the slopes (cf.
477 Fig. 10).
478 The mineralogical composition finally may give insight into the mechanisms of deposition and
479 transport present at this location. The DRIFT spectra allowed us to generally estimate mineral phases.
480 Quartz was recognised by the typical peak doublet at 780 and 800 cm^{-1}. The peaks at 3022, 2898,
481 2527, 1441, 1821, 822, 853 and 729 cm^{-1} are attributed to dolomite and those at 2893, 2875, 2513,
482 1796, 1430, 877, 848 and 713 cm^{-1} to calcite (Egli et al., 2008). Kaolinite is absent from the lake marl
483 (core G) but it was detected in the gyttja and soil profiles (Fig. 2). The gyttja layer of core B contained
484 major amounts mica (531 cm^{-1}), vermiculite, smectites and quartz, all of which are absent in the lake
485 marl or only marginally present in the limey gyttja of core C. By examining the peat layers using
486 DRIFT, we see that kaolinite is present throughout the whole peat body. Kaolinite also is enriched in
487 the topsoils and present in the mucks or gyttjas, but not in the lake marl. Mica is detected in both the
488 topsoils and mucks / gyttjas. The presence of the clay minerals generally points to the influence of
489 terrestrial weathering processes (Böhlert et al., 2011). It is highly likely that much of the kaolinite,
490 vermiculite and smectites were mechanically abraded from the parent material or soils and transported
491 into the mire (Last, 2002).
492
493 *4.3. Timing of the processes and landscape evolution*
494 The ages obtained from core G appear extraordinarily old (44500 cal BP and 42000 cal BP) in context
495 of a predominantly late-glacial sediment record here. However, two similar ages from the same
496 location from two independent samples lend much more credence that the ages accurately reflect the

existence of a lake in the basin prior to the LGM. Furthermore, no pollen was detected from the gyttia sediments (core G; depth 403 – 713 cm) which suggests that only sparse vegetation (if any) existed at this time. Thus, we suggest that an earlier lake existed here during an ice-free periglacial period prior to the LGM (Schlüchter et al., 1987; Schlüchter, 2004; Ivy-Ochs et al., 2006; Preusser, 2004; Hantke, 2011). The existence of an earlier lake is supported by Küttel and Lotter (1987) who suggested that a forest-free landscape existed in this region for the period 75 – 25 ka BP. We assume that the organic remnants isolated from core G from which our ^{14}C ages were derived (12700 cal BP and 10500 cal BP) probably were washed into the mire/lake from the surrounding vegetated slopes. The very low $\delta^{13}C$ values of -46‰ of these remnants probably point to the presence of archae/sulfate-reducing bacteria. Biogenic methane with $\delta^{13}C$ values between -50 to -110‰ is a potential source C source. Alperin and Hoehler (2009) showed that ^{13}C-depleted biomass and lipids observed in sediments from methane seep and vent sites may be derived from CO_2-reducing archaea and autotrophic sulfate-reducing bacteria.

Our data (based on the oldest age of the floating mat) indicate that post-LGM peat growth had started here by 11 ka BP. This gives a minimum-limiting age for peat formation but no information concerning how long the post-LGM lake may have existed before the peat began to form. According to Burga and Perret (1998), initial peat growth often started at the transition between Pleistocene and Holocene. Near the 10500 cal BP-dated limey gyttja layer (core BII) a subfossil leaf was found whose size and form suggest that shrubs (at least) were common in the region at this time. The pollens in the gyttja indicate a rather low percentage of non-arboreal vegetation and a multi-species forest with *Corylus avellana*, *Alnus*, *Ulmus*, *Quercus*, *Tilia* and some *Betula* and *Pinus*. Probably The forest may not have been very dense (due to a relatively low number of pollens) which suggests a late Preboreal/early Boreal open forest.

Sites containing *Pinus* and *Betula* tree species and *Juniperus* shrubs are known from this region during this period at slightly higher elevations (Küttel and Lotter, 1987; Gehrig, 1991; Burga and Perret, 1998). The presence of *Hedera helix* pollens at about 6 m depth indicated that the temperature of the

522 coldest month was not below zero or not much below zero (Iversen, 1944; Cheddadi et al., 1998).
523 Pollen analysed from 510 cm (core B) clearly indicates a warmer climate that can be attributed to the
524 Boreal or even early Atlanticum (Fagus) at about 10.2 to 9 ka BP. This does not totally align with the
525 associated C-14 age (10.5 to 11 ka BP) and may be due to the following reasons:
526 1. The deciduous forest developed in this area faster than previously suggested, or
527 2. this is a record of 'asynchronic' sedimentation of various compartments of gyttja: the organic matter
528 sampled for the C-14 ages was produced earlier as terrestrial material then transported/deposited later,
529 or
530 3. the gyttja started to form at 11000 cal BP, and its formation was prolonged until the Atlanticum. At
531 the same time, the 'floating mat' started to develop. Thus, the gyttja underlying the basal peat in core B
532 was deposited contemporaneously with the formation of the peat at water surface.
533 Later, the climate shifted to a warmer phase where deciduous species like *Corylus*, *Alnus*, *Ulmus*,
534 *Quercus* and *Tilia* were the main native vegetation. The ongoing growth of the floating mat seems to
535 have sustained shrubs at about 5000 cal BP (first woody peat layers on top of sedge peat). We know
536 that at this time the region was populated by deciduous forests of *Fagus*, *Picea* and *Pinus* (Küttel and
537 Lotter, 1987; Gehrig, 1991; Burga and Perret, 1998; Lotter, 1999). This can also be seen in our
538 palynological results, as we see *Picea abies* growing on the peat layer by about 2100 cal BP, a rather
539 common occurrence in the region at this time (Küttel and Lotter, 1987: Burga and Perret, 1998).
540 Continuous and progressive pedogenesis might be a justified assumption in some landscapes of long-
541 term geomorphic stability, e.g., old peneplains showing no substantial proisotropic pedoturbations. In
542 landscapes with a strong anthropogenic impact (e.g., intense historical land use), former periods of
543 geomorphic stability showing progressive soil development may be abruptly replaced by regressive
544 periods (e.g., Follain et al., 2006; Sommer et al., 2008). The regressive period is characterised by an
545 accelerated soil erosion/sedimentation due to clear-cutting or intensification of land use. Using the age
546 analyses of core C and the pollen data of core B, we see a major geosystem destabilisation with

increased erosion c. 4200 to 5000 cal BP, most likely due to human impact in the Neolithic or Early Bronze Age. Charcoal particles and other burnt organic remnants were found in all samples of the mire core section from 135 to 335 cm. At a depth of 335-344 cm only a few charcaol pieces (2-5%) were detected whereas the abundance was 15-40% at 275-284 cm and 5-15% at 210-215 cm. This may explain the high proportion of *Betula*, *Corylus* and *Filicales* (ferns). These plants are pioneer species that prefer open areas, and thus often appear in post-fire successions (Rackham, 1988; Göransson, 1994; Granoszewki, 2003). We see a significant increase in these species around 5000 cal BP. A similar effect was observed in an alpine lake in France (Brisset et al., 2013). According to Mourier et al. (2010) or Brisset et al. (2013), a stable landscape was interrupted by a major detrital pulse at 4200 cal BP that was considered as a tipping point in the environmental history of this area. At this point, pedogenetic processes drastically regressed, leading to the presence of moderately weathered soils. More frequent detrital inputs were recorded after 3000 cal BP as human impacts significantly increase in the catchment area of several alpine lakes (Brisset et al., 2013). Brisset et al. (2013) concluded that this destabilisation of the environment was triggered by climate and exacerbated by human activities to a stage beyond resilience. An increased input of inorganic components into the mire can be measured from about 2100 cal BP (Fig. 4). Since Roman time, human impact on soils and landscapes is an essential soil and landscape-forming factor. Studies of palaeosols, soil charcoal, or lacustrine sedimentary archives (e.g., Mourier et al. 2010) also confirm the succession of progressive (especially during the first part of the Holocene) and regressive soil formation phases even in Alpine areas (Egli and Poulenard, 2014).

5. Conclusions

The use of chemical tracers in lacustrine (lake or mire) sediments (Mourier et al., 2008, 2010; Brisset et al., 2013) has a great potential for deciphering characteristics of landscape history and soil evolution (weathering and erosion). Multi-elemental signatures allow us to discover important geochemical

processes that affect the development of regional and local landscapes. Together with radiocarbon and pollen analyses, the processes can be placed in a temporal context that allows us an extended interpretation of landscape dynamics.

The mire sediments reflect those stable phases (favourable for soil formation) of the surrounding area as well as unstable phases (leading to redistributions of sediment, e.g., erosion and sedimentation). Clearly, these redistribution phases were more intense at the margin of the mire and decreased towards the centre. Total elemental composition and REE were important tracers that allow us to differentiate between progressive and regressive phases of soil formation (Sommer et al., 2008).

A lake was already present in this region prior to the LGM (about 45000 cal BP; Fig. 11). After the LGM and associated deglaciation, the lake reappeared. Continuous sedimentation occurred until c. 11000 cal BP and the lake was mostly infilled with sediment by 11000 cal BP and a peat or a floating vegetation had started to build. A strong erosional phase occurred shortly after 11 ka BP. The duration of this erosion phase is unknown but assumed to be short. Thereafter, the landscape remained relatively stable between 11 – 2 ka BP (in the middle part of the mire; Fig. 11). At the margin of the mire, a more intense phase of sedimentation started c. 4000 cal BP pointing to a stronger period of slope erosion at this time. Roughly contemporaneous with the slope erosion (c. 5000 cal BP), we see a combination of vegetation clearing and fire events (evidently due to increasing human impact). This led to a shift of the vegetation composition for a longer period. Finally, geochemical and mineralogical tracers indicate a distinct period of soil erosion on the slopes with subsequent deposition of material in all areas of the mire about 2000 cal BP.

6. Acknowledgements

We would like to express our appreciation to B. Zollinger, K. Barmettler and S. Morganti for their assistance in the field and in the laboratory. We are, furthermore, indebted to two unknown reviewers

for their helpful comments on an earlier version of the manuscript. This research was supported by a grant from the Dienststelle für Umwelt und Energie, Kanton Luzern.

References

Adams, J.S., Kraus, M.J., Wing, S.L., 2011. Evaluating the use of weathering indices for determining mean annual precipitation in the ancient stratigraphic record. Palaeogeography, Palaeoclimatology, Palaeoecology 309, 358-366.

Aide, M., Smith-Aide, C., 2003. Assessing soil genesis by rare-earth elemental analysis. Soil Science Society of America Journal 67, 1470-1476.

Alperin, M.J., Hoehler, T.M., 2009. Anaerobic methane oxidation by archaea/sulfate-reducing bacteria aggregates: 2. Isotopic constraints. American Journal of Science 309, 958-984.

Anda, M., Chittleborough, D.J., Fitzpatrick, R.W., 2009. Assessing parent material uniformity of a red and black soil complex in the landscapes. Catena 78, 142-153.

Bennett, K.D., Willis, K.J., 2002. Pollen. In: Smol, J.P., Birks, H.J.B., Last, W.M. (Eds.), Tracking environmental change using lake sediments. Volume 3: Terrestrial, algal, and siliceous indicators. Kluwer Academic Publishers, New York, Boston, Dordrecht, pp. 5-32.

Bindler, R., Klaminder, J., 2006. Beyond the peat: synthesizing peat, lake sediments and soils in studies of the Swedish environment. In: Martini, I.P., Martínez Cortizas, A., Chesworth, W. (Eds.), Peatlands: Evolution and records of environmental and climate changes (Developments in Earth Surface Processes 9). Elsevier, Amsterdam, Boston, Heidelberg, pp. 431-448.

Birks, H.H., 2002. Plant macrofossils. In: Smol, J.P., Birks, H.J.B., Last, W.M. (Eds.), Tracking environmental change using lake sediments. Volume 3: Terrestrial, algal, and siliceous indicators. Kluwer Academic Publishers, New York, Boston, Dordrecht, pp. 49-74.

Böhlert, R., Mirabella, A., Plötze, M., Egli, M., 2011. Landscape evolution in Val Mulix, eastern Swiss Alps – Soil chemical and mineralogical analyses as age proxies. Catena 87, 313-325.

621 Boyle, J.F., 2002. Inorganic geochemical methods in Palaeolimnology. In: Last, W.M., Smol, J.P.
622 (Eds.), Tracking environmental change using lake sediments. Volume 2: Physical and geochemical
623 methods. Kluwer Academic Publishers, New York, Boston, Dordrecht, pp. 83-141.
624 Brisset, E., Miramont, C., Guiter, F., Anthony, E., Tachikawa, K., Poulenard, J., Arnaud, F., Delhon,
625 F., Meunier, J.-D., Bard E, Sumera, F., 2013. Non-reversible geosystem destabilisation at 4200
626 cal. BP: sedimentological, geochemical and botanical markers of soil erosion recorded in a
627 Mediterranean Alpine Lake. The Holocene 23, 1863-1874.
628 Bronk Ramsey, C., 2001. Development of the radiocarbon calibration program. Radiocarbon 43, 355-
629 363.
630 Bronk Ramsey, C., 2009. Bayesian analysis of radiocarbon dates. Radiocarbon 51, 337-360.
631 Buggle, B., Glaser, B., Hambach, U., Gerasimenko, N., Marković, S., 2011. An evaluation of
632 geochemical weathering indices in loess–paleosol studies. Quaternary International 240, 12-21.
633 Burga, C.A., Perret, R., 1998. Vegetation und Klima der Schweiz seit dem jüngeren Eiszeitalter. Ott
634 Verlag, Thun.
635 BWG (Bundesamt für Wasser und Geologie) (Ed.), 2006. Geologischer Atlas der Schweiz 1:25'000.
636 Atlasblatt 116 (Rigi – Blatt 1151 mit Nordteil von Blatt 1171 Beckenried) mit Erläuterungen von
637 R. Hantke. Bundesamt für Landestopographie Swisstopo, Bern.
638 Chadwick, O.A., Brimhall, G.H., Hendricks, D.M., 1990. From a black to a grey box – a mass balance
639 interpretation of pedogenensis. Geomorphology 3, 369-390.
640 Chapron, E., Faïn, X., Magand, O., Charlet, L., Debret, M., Mélières, M.A., 2007. Reconstructing
641 recent environmental changes from proglacial lake sediments in the Western Alps (Lake Blanc
642 Huez, 2543 m a.s.l., Grandes Rousses Massif, France). Palaeogeography, Palaeoclimatology,
643 Palaeoecology 252, 586-600.
644 Cheddadi R., Mamakowa K., Guiot J., de Beaulieu J.L., Reille M., Andrieu V., Granoszewski W.,
645 Peyron., 1998. Was the climate of the Eemian stable? A quantitative climate reconstruction from

seven European pollen records. Palaeogeography, Palaeoclimatology, Palaeoecology 143, 73-85.

Chmieleski, J., 2006. Zwischen Niedermoor und Boden: Pedogenetische Untersuchungen und Klassifikation von mitteleuropäischen Mudden. Dissertation Humboldt-Universität Berlin, Berlin.

Cohen, A.S., 2003. Paleolimnology. The history and evolution of lake systems. Oxford University Press, Oxford, New York.

Egli, M., Poulenard, J., 2014. Soils of Mountainous Landscapes. In: The International Encyclopedia of Geography" (Editor-in-chief Douglas Richardson; Physical Geography Editor Richard Marston), Wiley-Blackwell.

Egli, M., Brandova, D., Böhlert, R., Favilli, F., Kubik, P.W., 2010. ^{10}Be inventories in Alpine soils and their potential for dating land surfaces,. Geomorphology 119, 62-73.

Egli, M., Fitze, P., 2000. Formulation of pedologic mass balance based on immobile elements: a revision. Soil Science 165, 437-443.

Egli, M., Merkli, C., Sartori, G., Mirabella, A., Plötze, M., 2008. Weathering, mineralogical evolution and soil organic matter along a Holocene soil toposequence developed on carbonate-rich materials. Geomorphology 97, 675-696.

Egli, M., Zanelli, R., Kahr, G., Mirabella, A., Fitze, P., 2002. Soil evolution and development of the clay mineral assemblages of a Podzol and a Cambisol in 'Meggerwald', Switzerland. Clay Minerals 37, 337-352.

Erdtman G., 1960. The acetolysis method. Svensk Botanisk Tidskrift 54, 561-564.

Faegri K., Iversen J., 1989. Textbook of pollen analysis. Chichester, John Wiley.

Follain, S., Minasny, B., McBratney, A.B., Walter, C., 2006. Simulation of soil thickness evolution in a complex agricultural landscape at fine spatial and temporal scales. Geoderma 133, 71–86.

Franzén, L.G., 2006. Mineral matter, major elements, and trace elements in raised bog peat: a case study from southern Sweden, Ireland and Tierra del Fuego, south Argentina. In: Martini, I.P., Martínez Cortizas, A., Chesworth, W. (Eds.), Peatlands: Evolution and records of environmental

671 and climate changes (Developments in Earth Surface Processes 9). Elsevier, Amsterdam, Boston,
672 Heidelberg, pp. 241-269.
673 Gärtner, H., Lucchinetti, S., Schweingruber, F.H., 2014. New perspectives for wood anatomical
674 analysis in Dendrosciences: The GSL1-microtome. Dendrochronologia 32, 47-51.
675 Gehrig, R., 1991. Pollenanalytische Untersuchungen zur Vegetationsgeschichte des Pilatusgebietes.
676 Mitteilungen der Naturforschenden Gesellschaft Luzern 32, 128-143.
677 GKSNG (Geologische Kommission der Schweizerischen Naturforschenden Gesellschaft), Swisstopo
678 (Bundesamt für Landestopografie) (Eds.), 1962. Geologischer Atlas der Schweiz 1:25'000.
679 Erläuterungen zu Atlasblatt 28 (Luzern – Blätter 202 Rothenburg, 203 Emmen, 204 Malters, 205
680 Luzern). Kümmerly & Frey Geographischer Verlag, Bern.
681 Göransson H., 1994. Comments on Neolithic farming practice – An archaeological response to the
682 Göransson hypothesis. Fornvännen 89, 168-184.
683 Granoszewski W., 2003. Late Pleistocene vegetation history and climatic changes at Horoszki Duże,
684 eastern Poland: a palaeobotanical study. Acta Palaeobotanica suppl. 4, 3-95.
685 Guha, H., Saiers, J.E., Brooks, S., Jardine, P., Jayachandran, K., 2001. Chromium transport, oxidation,
686 and adsorption in manganese-coated sand. Journal of Contaminant Hydrology 49, 311-334.
687 Hantke, R., 1967. Geologische Karte des Kantons Zürich und seiner Nachbargebiete in 2 Blättern
688 1:50'000 mit Erläuterungen. Vierteljahrsschrift der Naturforschenden Gesellschaft in Zürich, 112.
689 Hantke, R., 1980. Eiszeitalter. Die jüngste Erdgeschichte der Schweiz und ihrer Nachbargebiete. Band
690 2: Letzte Warmzeiten, Würm-Eiszeit, Eisabbau, Nacheiszeit der Alpen-Nordseite vom Rhein- zum
691 Rhone-System. Ott Verlag, Thun.
692 Hantke, R., 2011. Eiszeitalter. Kalt- /Warmzeit-Zyklen und Eistransport im alpinen und voralpinen
693 Raum. Hep Verlag, Bern.
694 Hitz, C., Egli, M., Fitze, P., 2002. Determination of the sampling volume for representative analysis of
695 alpine soils. Zeitschrift für Pflanzenernährung und Bodenkunde 165, 326-331.

696 Ingri, J., Widerlund, A., Land, M., Gustafsson, O., Andersson, P., Öhlander, B., 2000. Temporal
697 variations in the fractionation of the rare earth elements in a boreal river; the role of colloidal
698 particles. Chemical Geology 166, 23–45.
699 IUSS Working Group WRB, 2007. World Reference Base for Soil Resources (2nd ed.). World Soil
700 Resources Reports No. 103, First update, FAO, Rome.
701 Iversen J., 1944. Viscum, Hedera and Ilex as climate indicators. A contribution to the study of Post-
702 Glacial temperature climate. Geol. Foren. Forhlandl. 666, 464-483.
703 Ivy-Ochs, S., Kerschner, H., Reuther, A., Maisch, M., Sailer, R., Schaefer, J., Kubik, P.W., Synal, H.-
704 A., Schlüchter, C., 2006. The timing of glacier advances in the northern European Alps based on
705 surface exposure dating with cosmogenic ^{10}Be, ^{26}Al, ^{36}Cl, and ^{21}Ne. Geological Society of
706 America Special Paper 415, 43-60.
707 Johnson, D.L.,Watson-Stegner, D., 1987. Evolution model of pedogenesis. Soil Science 143, 349–366.
708 Küttel, M., Lotter, A.F., 1987. Vegetation und Landschaft der Zentralschweiz im Jungpleistozän.
709 Mitteilungen der Naturforschenden Gesellschaft Luzern 29, 251-272.
710 Last, W.M., 2002. Mineralogical analysis of lake sediments. In: Last, W.M., Smol, J.P. (Eds.),
711 Tracking environmental change using lake sediments. Volume 2: Physical and geochemical
712 methods. Kluwer Academic Publishers, New York, Boston, Dordrecht, pp. 143-187.
713 Le Roux, G., Shotyk, W., 2006. Weathering of inorganic matter in bogs. In: Martini, I.P., Martínez
714 Cortizas, A., Chesworth, W. (Eds.), Peatlands: Evolution and records of environmental and
715 climate changes. Elsevier, Amsterdam, Boston, Heidelberg, pp. 197-215.
716 Lotter, A. F., 1999. Late-glacial and Holocene vegetation history and dynamics as shown by pollen
717 and plant macrofossil analyses in annually laminated sediments from Soppensee, Central
718 Switzerland. Vegetation History and Archeobotany, 8, 165-184.
719 Lotter, A.F., Zbinden, H., 1989. Late-glacial pollen analysis, oxygen-isotope record, and radiocarbon
720 stratigraphy from Rotsee (Lucerne), Central Swiss Plateau. Eclogae geologicae Helvetiae 82, 191-

721 202.
722 Mondal, M.E.A., Wani, H., Mondal, B., 2012. Geochemical signature of provenance, tectonics and
723 chemical weathering in the Quaternary flood plain sediments of the Hindon River, Gangetic plain,
724 India. Tectonophysics 566-567, 87-94.
725 Mourier, B., Poulenard, J., Carcaillet, C., Williamson, D., 2010. Soil evolution and subalpine
726 ecosystem changes in the French Alps inferred from geochemical analysis of lacustrine sediments.
727 Journal of Paleolimnology 44, 571-587.
728 Mourier, B., Poulenard, J., Chauvel, C., Faivre, P., Carcaillet, C., 2008. Distinguishing subalpine soil
729 types using extractible Al and Fe fractions and REE geochemistry. Geoderma 145, 107-120.
730 Mühlethaler, E., 2002. Nutzungsgeschichte der Flachmoore in der Schweiz. In: Bundesamt für Umwelt
731 Wald und Landschaft BUWAL (Ed.), Handbuch Moorschutz in der Schweiz 1. BUWAL, Bern,
732 pp. 3.2.3.
733 Nalepka D., Walanus A., 2003. Data processing in pollen analysis. Acta Palaeobotanica 43, 125-134.
734 Öhlander, B., Land, M., Ingri, J., Widerlund, A., 1996. Mobility of rare earth elements during
735 weathering of till in northern Sweden. Applied Geochemistry 11, 93-99.
736 Preusser, F., 2004. Towards a chronology of the Late Pleistocene in the northern Alpine Foreland.
737 Boreas 33, 195-210.
738 Preusser, F., Graf, H.R., Keller, O., Krayss, E., Schlüchter, C., 2011. Quaternary glaciation history of
739 northern Switzerland. Quaternary Science Journal 60, 282-305.
740 Probst, E., 1922. Die Torfausbeutung in der Schweiz in den Jahren 1917 bis 1921. Eidgenössische
741 Inspektion für Forstwesen, Jagd und Fischerei, Bern.
742 Rackham O., 1988. Trees and woodland in a crowded landscape – the cultural landscape of the British
743 Isles. In: Birks, H.H., Birks, H. J. B., Kaland, P. E., Moe, D. (Eds.), The Cultural Landscape, Past,
744 Present and Future. Cambridge University Press, Cambridge, pp. 53-78.

745 Reimer, P.J., Baillie, M.G.L., Bard, E., Bayliss, A., Beck, J.W., Blackwell, P.G., Bronk Ramsey, C.,
746 Buck, C.E., Burr, G.S., Edwards, R.L., Friedrich, M., Grootes, P.M., Guilderson, T.P., Hajdas, I.,
747 Heaton, T.J., Hogg, A.G., Hughen, K.A., Kaiser, K.F., Kromer, B., McCormac, F.G., Manning,
748 S.W., Reimer, R.W., Richards, D.A., Southon, J.R., Talamo, S., Turney, C.S.M., van der Plicht, J.,
749 Weyhenmeyer, C.E., 2009. INTCAL09 and MARINE09 radiocarbon age calibration curves, 0-
750 50,000 years cal BP. Radiocarbon 51, 1111-1150.
751 Richardson, J., Vepraskas, M., 2001. Wetland Soils: Genesis, Hydrology, Landscapes and
752 Classification. Lewis Publishers, Boca Raton, London, New York, pp. 417.
753 Rinklebe, J., Shaheen, S.M., 2014. Assessing the mobilization of cadmium, lead, and nickel using a
754 seven-step sequential extraction technique in contaminated floodplain soil profiles along the
755 central Elbe river, Germany. Water, Air, and Soil Pollution 225, DOI 10.1007/s11270-014-2039-
756 1.
757 Röösli, T., Bolzern, H., Borgula, A., 2004. Schutz-, Pflege- und Aufwertungskonzept Moosried.
758 Naturschutzwerte, Schutz und Entwicklungsziele, Massnahmen. Amt für Natur- und
759 Landschaftsschutz, Luzern.
760 Rydin, H., Jeglum, J., 2006. The Biology of Peatlands (Biology of Habitats Series). Oxford University
761 Press, Oxford, New York.
762 Schlüchter, C., 2004. The Swiss glacial record – A schematic summary. In: Ehlers, J., Gibbard, P.L.
763 (Eds.), Quaternary Glaciations – Extent and Chronology. Elsevier, Amsterdam, Boston,
764 Heidelberg, pp. 413-418.
765 Schlüchter, C., Maisch, M., Suter, J., Fitze, P., Keller, W.A., Burga, C.A., Wynistorf, E., 1987. Das
766 Schieferkohlen-Profil von Gossau (Kanton Zürich) und seine stratigraphische Stellung innerhalb
767 der letzten Eiszeit. Vierteljahrsschrift der Naturforschenden Gesellschaft in Zürich 132, 135-174.
768 Schweingruber, F.H., 1990. Mikroskopische Holzanatomie. Swiss Federal Institute for Forest, Snow
769 and Landscape Research WSL, Birmensdorf.

770 Schweingruber, F.H., 1996. Tree rings and environment. Dendroecology. Swiss Federal Institute for
771 Forest, Snow and Landscape Research WSL / Haupt Verlag, Birmensdorf / Bern.
772 Sommer, M., Halm, D., Geisinger, C., Andruschkewitsch, I., Zarei, M., Stahr, K., 2001. Lateral
773 podzolization in a sandstone catchment. Geoderma 103, 231-247.
774 Sommer, M., Gerke, H.H., Deumlich, D., 2008. Modelling soil landscape genesis – A "time split"
775 approach for hummocky agricultural landscapes. Geoderma 145, 480-493.
776 Stanin, F.T, Pirnie, M., 2004. The Transport and Fate of Cr(VI) in the Environment. In: Guertin, J.,
777 Jacobs, J.A., Avakian, C.P. (Eds.), Chromium(VI) Handbook, CRC Press, pp. 161-211.
778 Stutter, M.I., Langan, S.J., Lumsdon, D.G., Clark, L.M., 2009. Multi-element signatures of stream
779 sediments and sources under moderate to low flow conditions. Applied Geochemistry 24, 800-
780 809.
781 Succow, M., Joosten, H., 2001. Landschaftsökologische Moorkunde. E. Schweizerbart'sche
782 Verlagsbuchhandlung, Stuttgart.
783 Sun, S.S., McDonough, W.F., 1989. Chemical and isotopic systematics of oceanic basalts:
784 implications for mantle composition and processes. In: Saunder, A.D., Norry, M.J. (Eds.),
785 Magmatism in oceanic basins. Special publication 42. Geological Society of London, London, pp.
786 313-345.
787 Taylor, S.R., McLennan, S.M., 1985. The continental crust: Its composition and evolution. Blackwell,
788 Oxford.
789 Taylor, S.R., McLennan, S.M., 1995. The geochemical evolution of the continental crust. Reviews of
790 Geophysics, 33, 241-265.

Table 1
Click here to download Table: Table_1.doc

Table 1. Characteristics of the sampling sites.

Profile	Coordinates WGS 84 (N/E)	Elevation m asl	Site	Vegetation	Slope	Exposure °N	Sampling depth (cm)	Soil order (IUSS working group, 2007)
Soil profiles								
P1	47°04'32"/08°23'35"	571	Stotziglauf	Coniferous forest	15°	340	0-100	Dystric Cambisol
P2	47°04'34"/08°23'36"	557	Stotziglauf	Coniferous forest	36°	320	0-100	Dystric Cambisol
P3	47°04'33"/08°23'31"	542	Moosried	Wet meadow	26°	310	0-100	Mollic Gleysol
Mire cores								
A	47°04'36"/08°23'29"	540	Moosried	Sedge reed	0	-	0-265	Fibric Histosol
B	47°04'36"/08°23'26"	540	Moosried	Sedge reed	0	-	0-220	Fibric Histosol
B II	47°04'36"/08°23'26"	540	Moosried	Sedge reed	0	-	257-704	Fibric Histosol
C	47°04'32"/08°23'30"	542	Moosried	Wet meadow	1	305	0-360	Fibric Histosol
E	47°04'35"/08°23'36"	547	Moosried	Wet meadow	2	305	0-385	Mollic Gleysol
EXK	47°04'35"/08°23'28"	540	Moosried	Wet meadow	0	-	102-132	Fibric Histosol
G	47°04'35"/08°23'28"	540	Moosried	Wet meadow	0	-	112-713	Fibric Histosol

Table 2
Click here to download Table: Table_2.doc

Table 2. Some typical properties of the investigated soils.

Profile	Horizon	Depth cm	Bulk density (g/cm^3)	LOI (%)	pH ($CaCl_2$)	Skeleton (vol.-%)	Munsell colour (moist)
Profile 1	O	0-7	0.67	27	3.25	5%	7.5YR 2/1
	AE	7-25	0.74	16	3.70	5%	7.5 YR 4/2
	Bsw	25-50	0.70	9	4.50	20%	10YR 5/8
	BC	50-80	1.30	4	5.00	20%	2.5YR 5/6
	R	80-100	-	-	-	>50%	-
Profile 2	O	0-5	0.54	22	3.50	2%	7.5YR 3/2
	AE	5-15	0.73	10	4.00	2%	7.5 YR 4/2
	Bws	15-30	0.80	9	4.40	2%	7.5YR 5/4
	Bw	30-90	1.35	5	4.80	5%	10YR 5/8
	BC	90-100	1.65	3	5.50	5%	10YR 6/4
Profile 3	A	0-25	1.09	8	5.10	0%	10YR 3/3
	Bl	25-80	1.69	4	5.80	5%	2.5Y 5/2
	Cr	80-100	1.66	5	6.45	5%	2.5Y 5/2

Table 3
Click here to download Table: Table_3.doc

Table 3. Total elemental contents of the soil samples.

Profile	Horizon	Depth cm	Ca g/kg	Mg g/kg	K g/kg	Na g/kg	Si g/kg	Al g/kg	Fe g/kg	Mn g/kg	Ti g/kg	Zr g/kg	La g/kg	Ce g/kg	Pr g/kg	Nd g/kg	Sm g/kg
Profile 1	O	0-7	1.46	4.76	15.49	12.94	263	49.29	12.50	0.073	2.17	0.129	0.008	0.021	0.000	0.000	0.000
	AE	7-25	1.33	5.18	17.56	12.43	295	55.84	17.49	0.081	2.30	0.149	0.010	0.022	0.000	0.011	0.000
	Bsw	25-50	1.48	6.39	20.32	13.31	318	70.33	17.79	0.135	2.30	0.143	0.010	0.028	0.000	0.012	0.000
	BC	50-80	1.74	10.10	28.76	21.45	300	85.87	13.17	0.254	1.56	0.083	0.016	0.037	0.011	0.017	0.000
Profile 2	O	0-5	1.03	5.73	16.29	11.30	264	55.99	15.32	0.078	2.20	0.136	0.015	0.029	0.010	0.019	0.000
	AE	5-15	1.12	6.26	19.84	12.43	310	63.70	17.81	0.086	2.42	0.149	0.011	0.028	0.005	0.009	0.000
	Bws	15-30	1.15	6.15	20.54	14.16	314	69.42	17.86	0.101	2.33	0.158	0.010	0.029	0.000	0.008	0.000
	Bw	30-90	1.27	7.85	23.46	15.46	334	75.78	16.74	0.189	2.33	0.146	0.011	0.034	0.005	0.011	0.000
	BC	90-100	1.54	9.30	31.08	20.16	306	80.51	15.85	0. 229	2.24	0.135	0.012	0.039	0.006	0.014	0.000
Profile 3	A	0-25	3.37	7.34	22.03	10.86	292	58.66	17.47	0.358	2.68	0.143	0.015	0.035	0.000	0.017	0.000
	Bl	25-80	3.78	14.68	25.52	13.16	326	77.19	21.12	0.203	3.03	0.152	0.017	0.040	0.007	0.022	0.000
	Cr	80-100	3.90	13.48	25.78	13.48	320	77.75	20.79	0.211	3.03	0.132	0.017	0.048	0.007	0.023	0.000

Table 4
Click here to download Table: Table_4.doc

Table 4. Radiocarbon dating of the mire samples

Sample	Code	Depth (cm)	Material	BP uncal	$\delta^{13}C$	cal BP (1 σ range)
hjB2c	UZ-6118/ETH-48768	35–40	Peat	2135 ± 25	-26.98 ±1.1‰	2285 – 2061
hjB9c	UZ-6119/ETH-48769	210–215	Wood	4395 ± 25	-27.55 ±1.1‰	5033 – 4879
hjBII4e	UZ-6060/ETH-46230	354–363	Peat base	9530 ± 40	-27.70 ±1.1‰	11068 – 10720
hjBII11d	UZ-6058/ETH-46228	695–704	Sediment	9410 ± 40	-29.80 ±1.1‰	10688 – 10586
hjC4e	UZ-6120/ETH-48770	95–100	Wood	3665 ± 25	-30.60 ±1.1‰	4076 – 3929
hjC15a	UZ-6059/ETH-46229	350–355	Peat base	4680 ± 30	-26.40 ±1.1‰	5465 – 5325
hjEXK1	UZ-6078/ETH-46968	112	Peat base	8465 ± 35	-29.30 ±1.1‰	9520 – 9472
hjG5d/6e	UZ-6176/ETH-52558	345-413	Organic remants	10820 ± 60	-46.10 ±1.1‰	12758 – 12612
hjG7b/8e	ZU-6177/ETH-52559	426-485	Organic remants	9300 ± 50	-45.70 ±1.1‰	10575 – 10420
hjG6e	UZ-6116/ETH-48766	404–413	Sediment	37140 ± 190	- 0.28 ±1.1‰	42157 – 41775
hjG12e	UZ-6117/ETH-48767	704–713	Sediment	40880 ± 335	- 0.40 ±1.1‰	44913 – 44355

Table 5
Click here to download Table: Table_5.doc

Table 5. Chondrite normalised REE for some core and soil profile layers.

Chondrite normalised REE						
Site	Depth (cm)	La	Ce	Pr	Nd	Sm
		Conc. measured / Conc. chondrite				
BII	495-504	0.012	0.008	0.017	0.006	0.006
C	300-305	0.006	0.005	0.008	0.003	0.000
C	350-355	0.002	0.001	0.000	0.000	0.009
E	300-305	0.011	0.009	0.007	0.006	0.000
G	494-504	0.009	0.008	0.000	0.004	0.008
P1	80-100	0.007	0.006	0.012	0.004	0.000
P2	90-100	0.005	0.006	0.006	0.003	0.000
P3	80-100	0.007	0.008	0.007	0.005	0.000

Figure captions

Fig. 1. Location of the investigation area and sampling sites. P1-3 are soil profiles and A, B, BII, C, E, G, Exk profiles in the mire. B/BII and G/Exk are complementary drillings next to each other.

Fig. 2. DRIFT diagrams of selected samples showing typical material properties of the mire cores and soils.

Top left: Horizons of soil profile 2 – O, AE, Bws, Bw and BC (from the top). Top right: Lowermost soil horizons and core E – profile 1 with horizon BC, profile 2 with horizon BC, profile 3 with horizon Cr, core E (200 – 205 cm depth) (from the top). Lower left: Core G – lake marl (112 – 121 cm depth), marly silt (295 – 304 cm depth), clayey silt (495 – 604 cm depth) (from the top). Lower right: Assembled peat cores – core A (25 – 30 cm depth), core B (100 – 105 cm depth), core BII (495 – 504 cm depth), core BII (695 – 704 cm depth) (from the top).

Fig. 3. Bulk density and pH along the cores B/BII, C, E and G.

Fig. 4. LOI (loss on ignition), carbonate (E und G), SiO_2 and Al_2O_3 concentrations for the mire cores B/BII, C, E and G. Age indications are given for the cores B/BII and C.

Fig. 5. Cross section of *Picea abies* root remains found in core B (40 – 45 cm depth). The root remains are slightly younger (found just above a dated layer; Fig. 6) than 2285 – 2061 cal BP (Sub-Atlantic).

Left: Frost-ring detectable in the 3rd year (magnification 30x), Right: compression wood (magnification 30x).

Fig. 6. Cross-section of the mire (scheme based on Succow and Joosten, 2001) together with the measured C-14 ages.

Fig. 7. Pollen spectra along core B/BII.

Fig. 8. UCC normalized major and trace elements.

Fig. 9. Open-system mass transport function (τ) for major elements along the soil profiles. The arrow indicates the mass flow from P1 to P3. Soil horizons are also given for the first graph.

Fig. 10. Open-system mass transport function (τ) for the sum of measured rare earth elements (REE) along the soil profiles and mire cores. The dashed arrow indicates the direction from the slope towards the middle of the mire.

Fig. 11. Hypothesised schemes of landscape dynamics of the investigation area during the late Pleistocene and Holocene.

Figure 1

Click here to download high resolution image

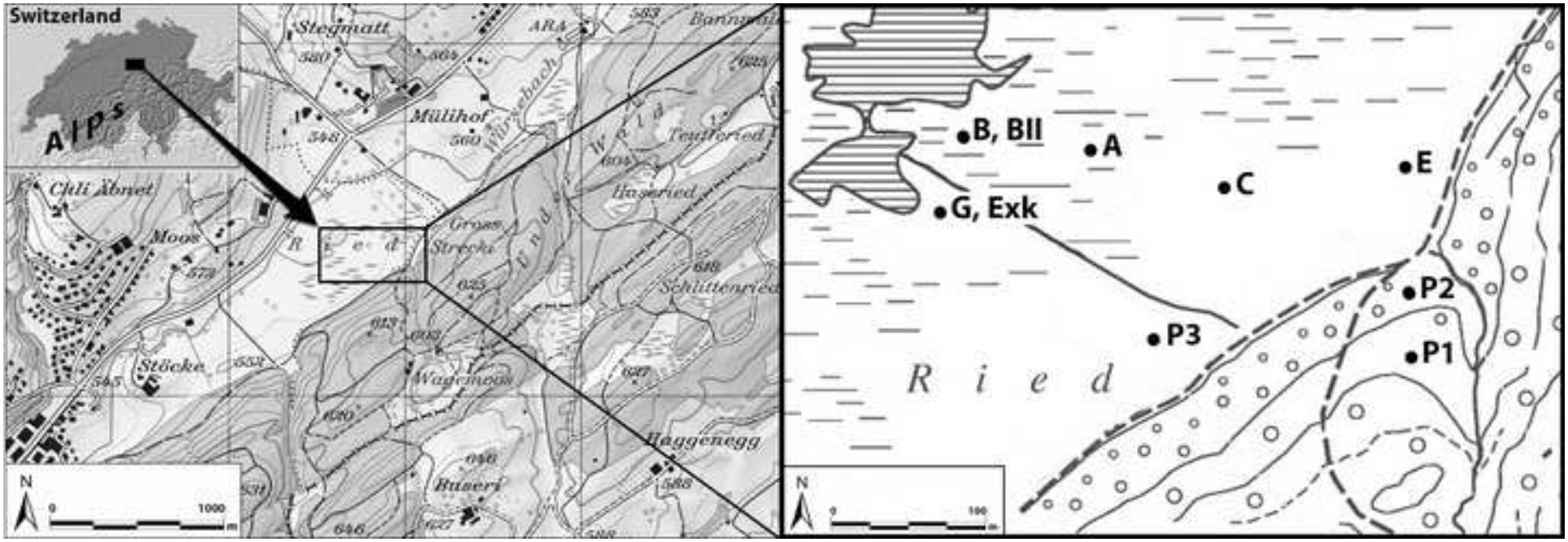

Figure 2

Click here to download high resolution image

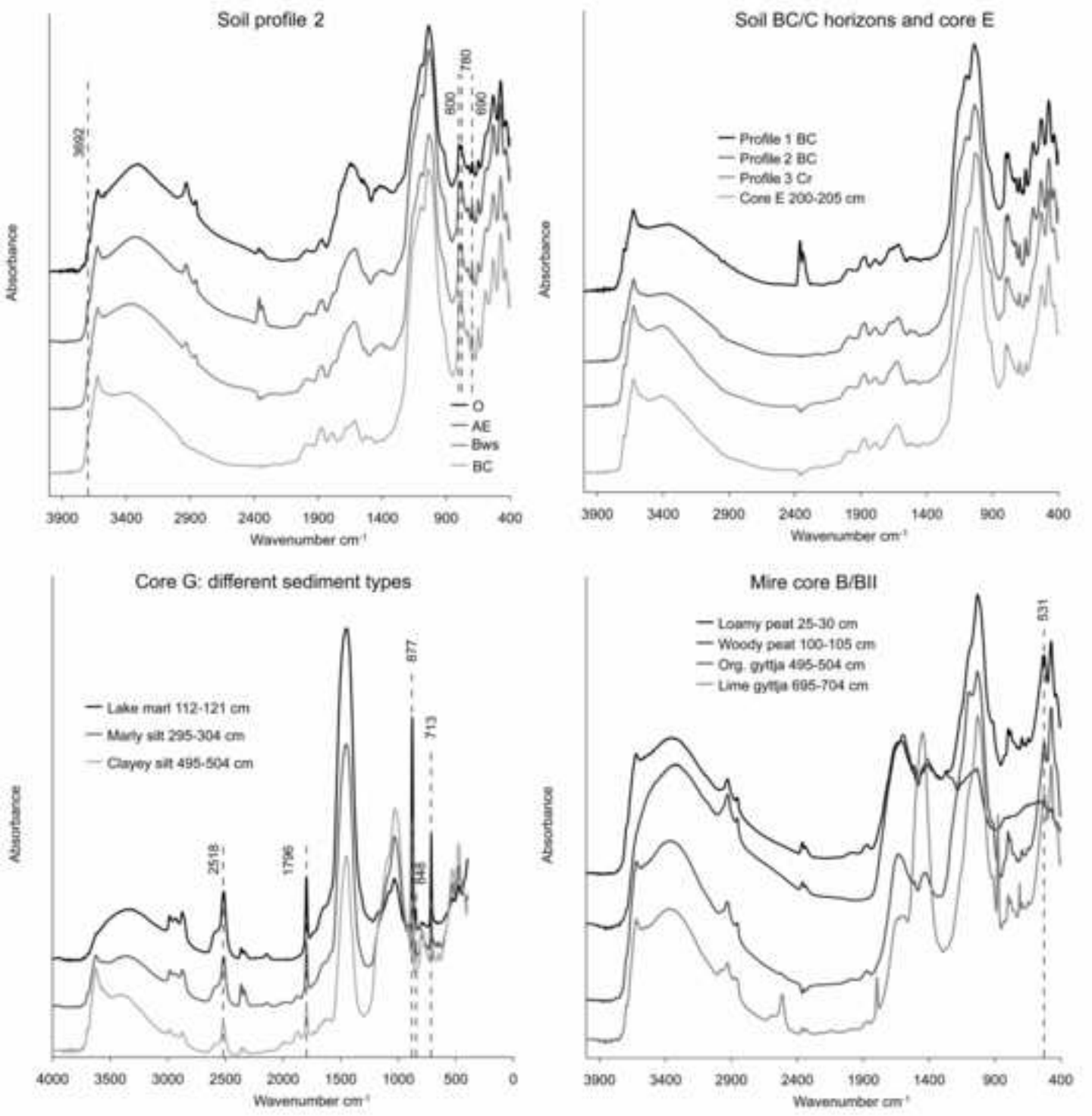

Figure 3

Click here to download high resolution image

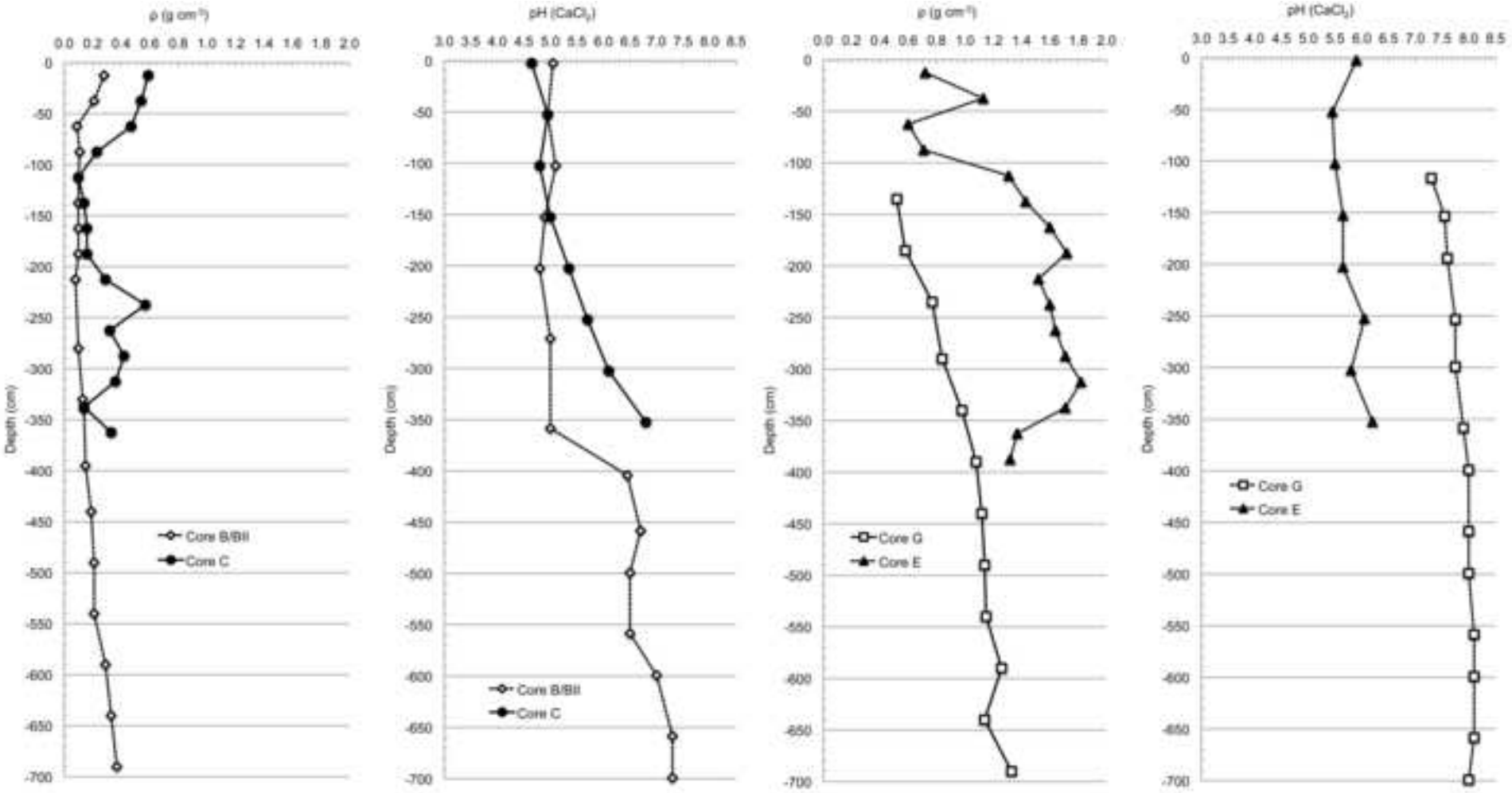

Figure 4

Click here to download high resolution image

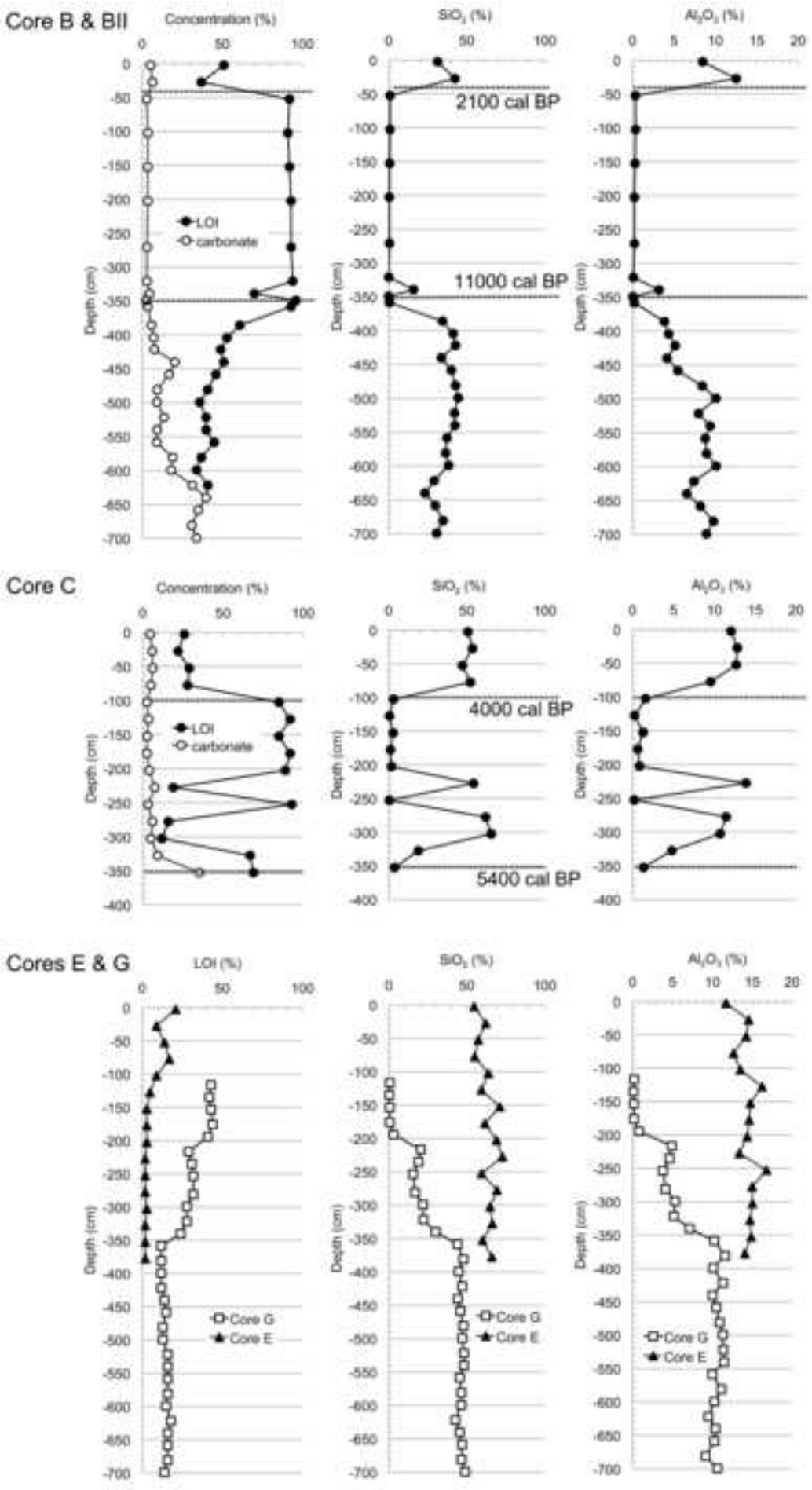

Figure 5

Click here to download high resolution image

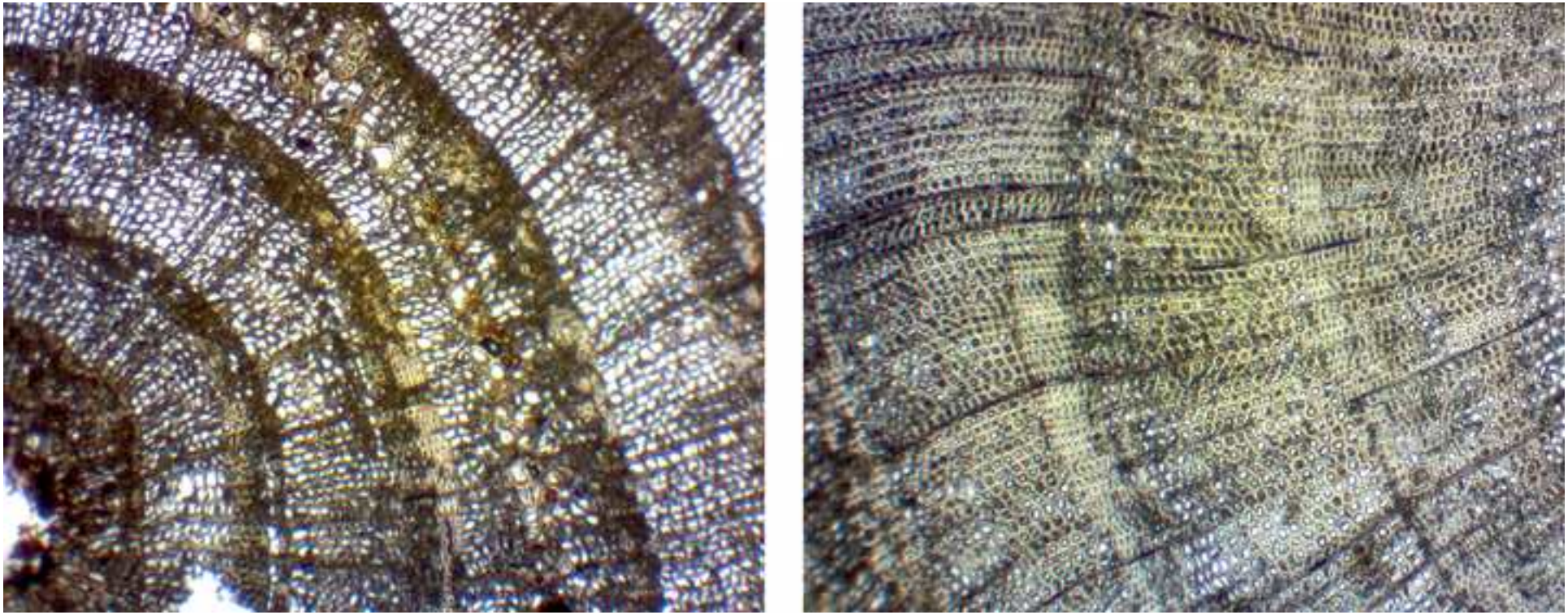

Figure 6

Click here to download high resolution image

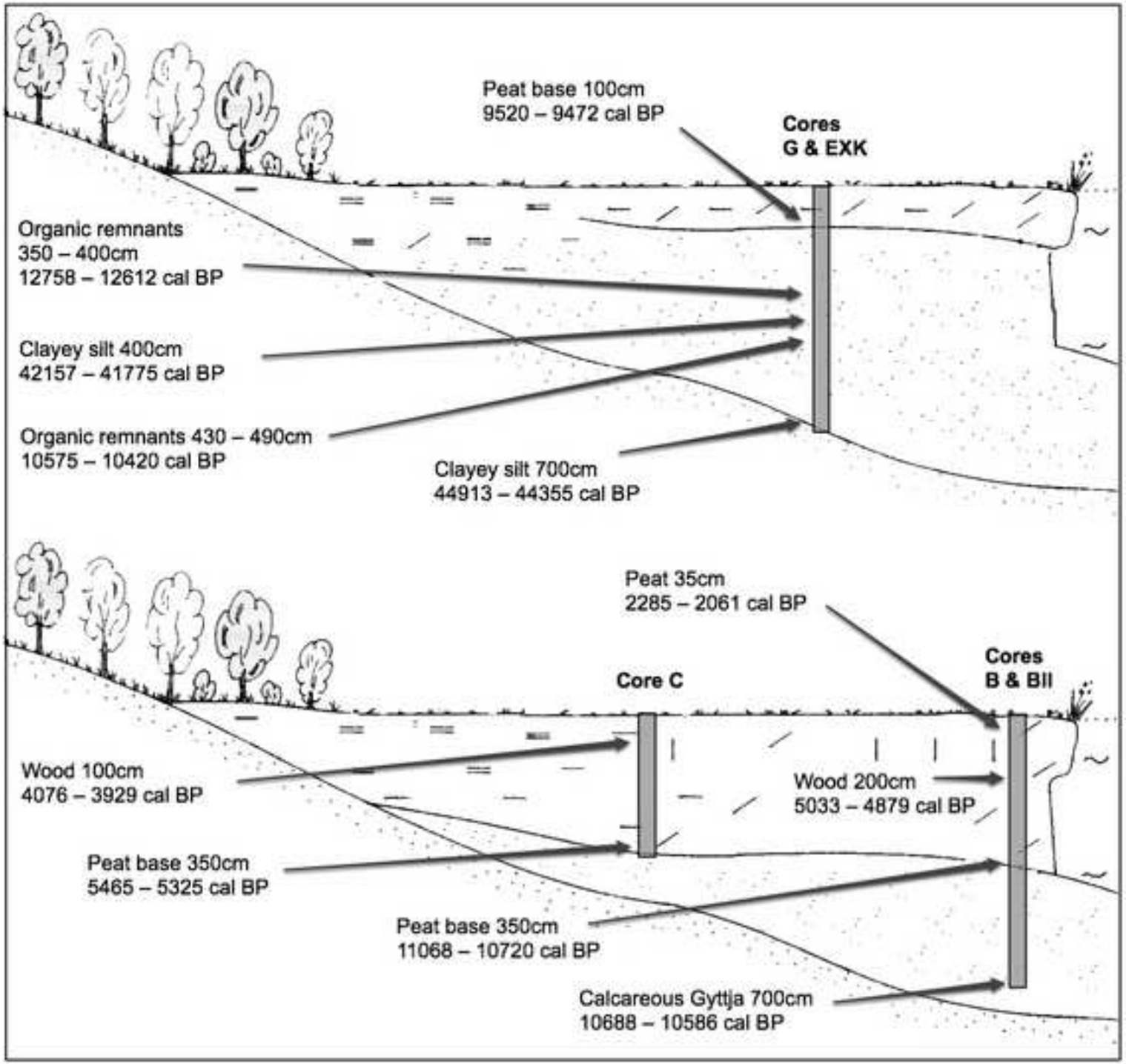

Figure 7

Click here to download high resolution image

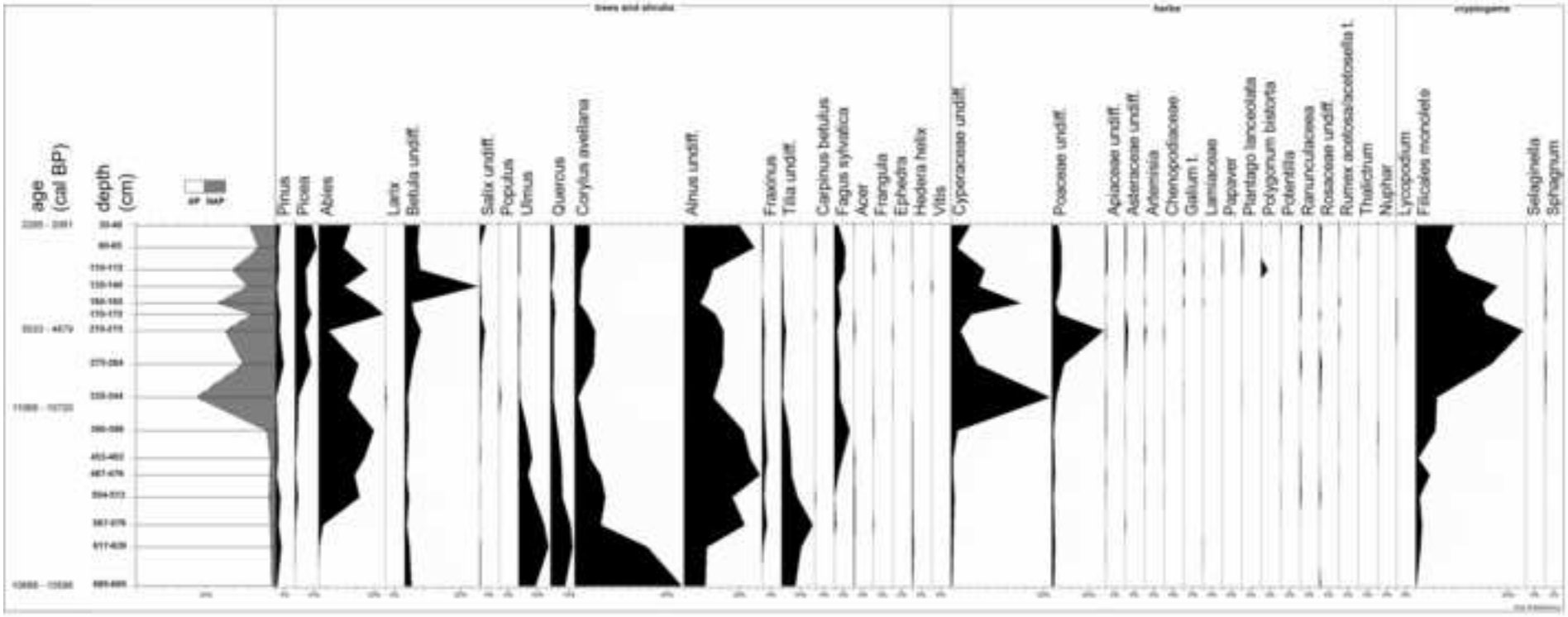

Figure 8

Click here to download high resolution image

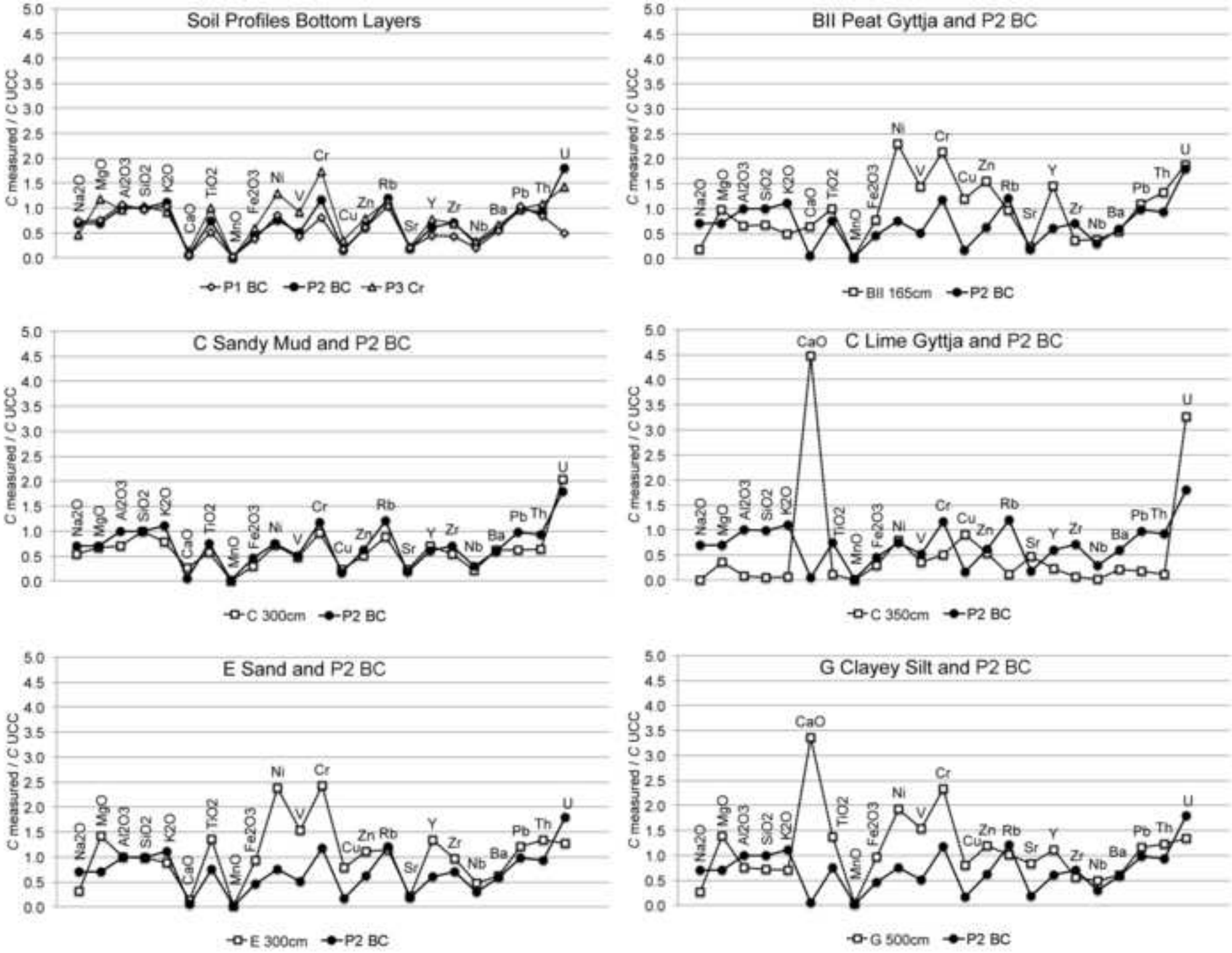

Figure 9

Click here to download high resolution image

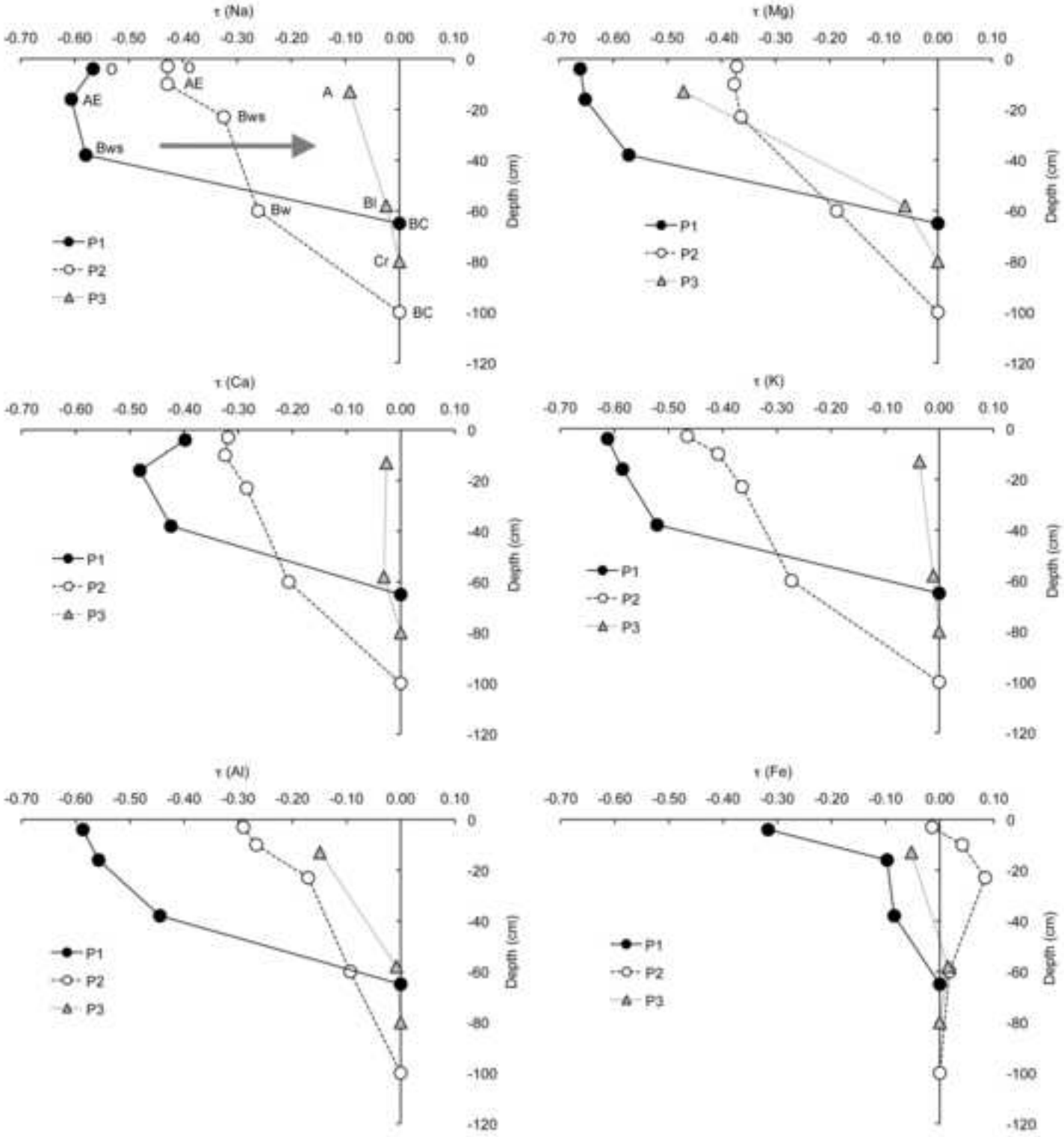

Figure 10

Click here to download high resolution image

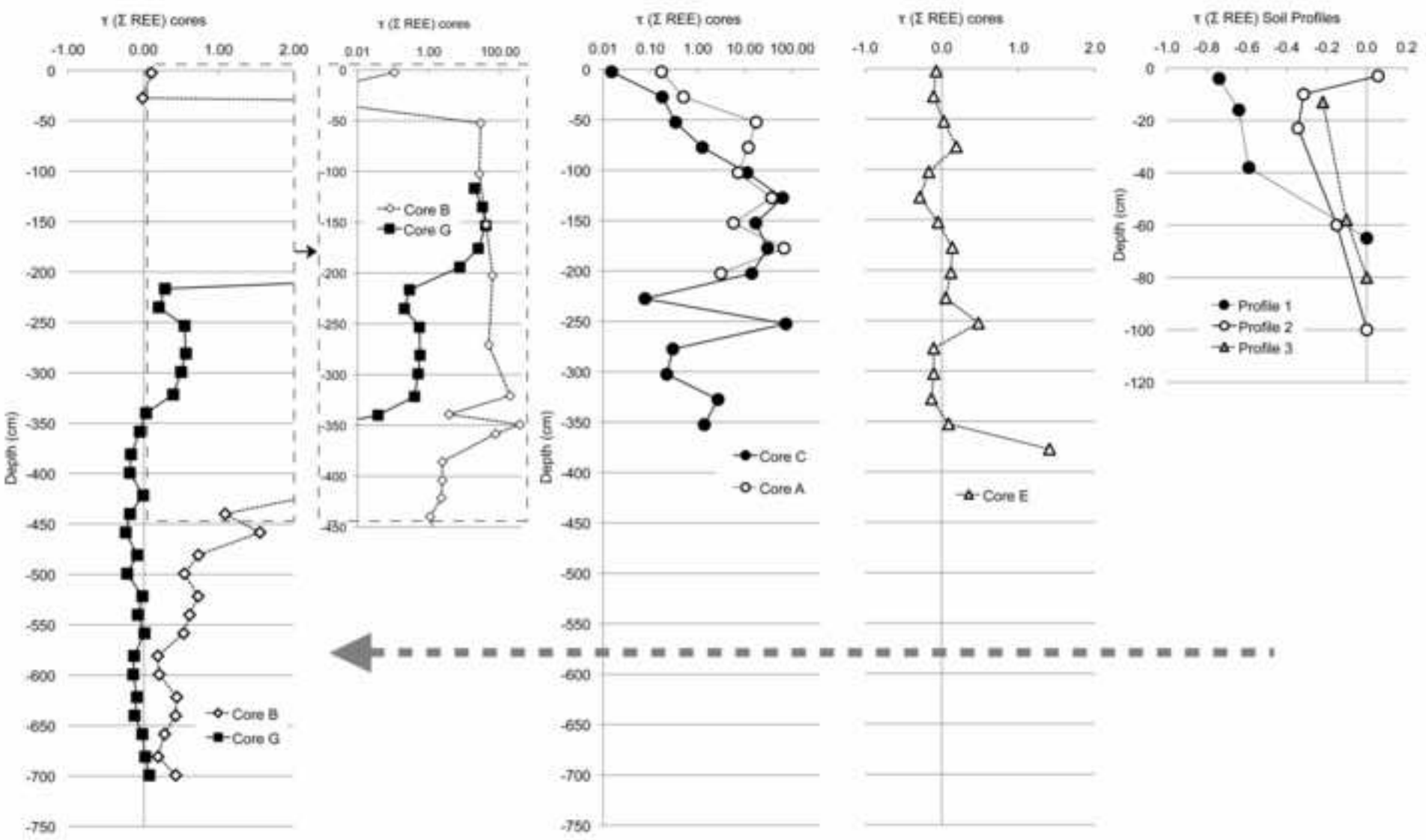

Figure 11

Click here to download high resolution image